



Next Generation Space Telescope

NGST

A NASA  
Origins  
Mission

# NGST Wavefront Sensing and Control

August 25, 2002

David Redding, Scott Basinger, David Cohen, Joseph Green,  
Andrew Lowman, Catherine Ohara, Fang Shi

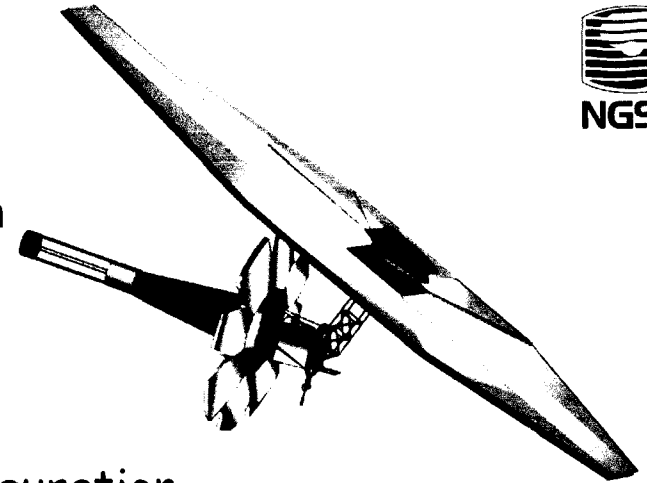
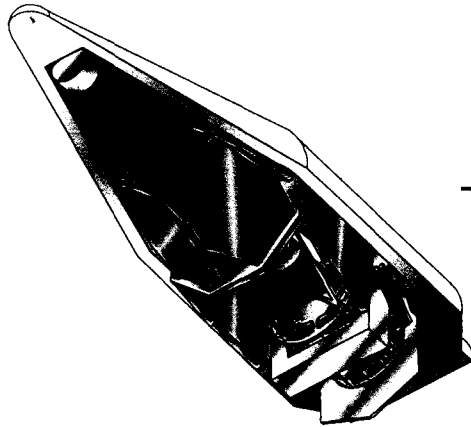
Jet Propulsion Laboratory, California Institute of Technology

Charles Bowers, Richard Burg, Laura Burns, Bruce Dean, Peter  
Petrone

NASA Goddard Space Flight Center

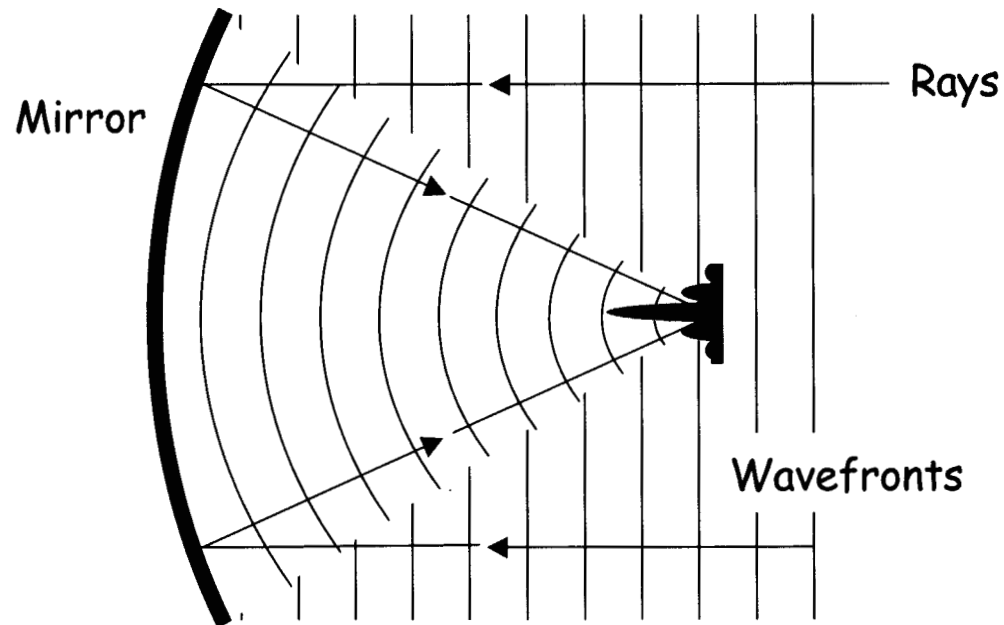
# NGST Yardstick

The "Government Team" point design  
for feasibility and other studies:  
Soon to be supplanted by a  
Prime Contractor design!



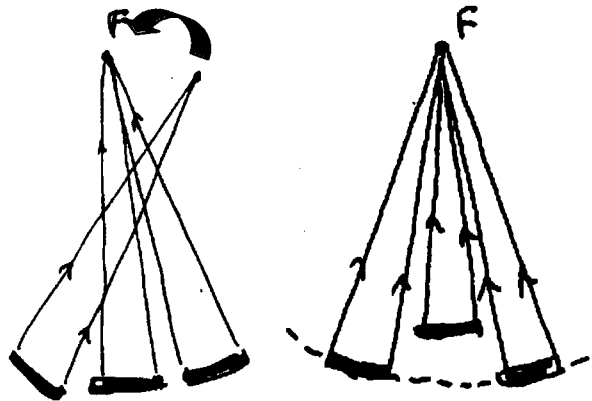
- Nine rigid segments in a "flower" configuration
- Segments cryo-figured to under 1 wave ( $\lambda = 2$  mm) at operating temperature
- Segments and SM deployed to 5 mm piston, 5 mrad tilt accuracy
- Segments actuated in rigid-body DOFs
- Deformable quaternary mirror provides means of correcting segment figure errors
- NIR and MIR cameras provide 1-16 mm imaging, can be used for WF sensing
- Very low temperature change across operating envelope
- Very low effective system CTE (may include active thermal control)
- Very low vibration and slew environment

# Imaging and Wavefront Control



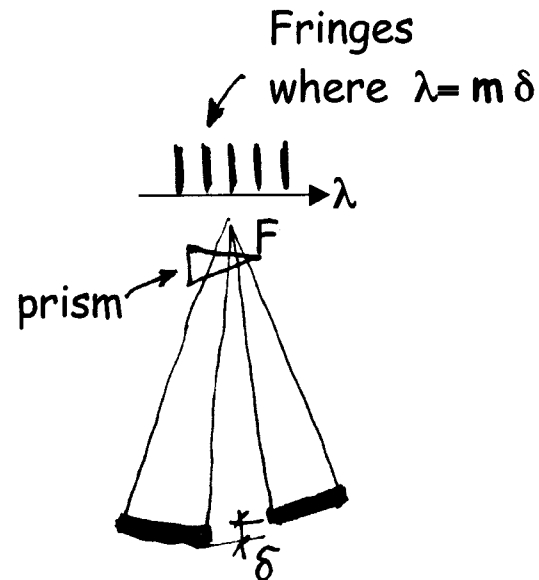
- A perfect optical system converts incoming wavefronts to concentric spherical wavefronts converging to a point image on a detector
- Imperfections arise from fabrication error, temperature changes, alignment shifts, strain relief, long-term dimensional change
  - Traditionally minimized using massive structures
- Wavefront control uses moving and deforming elements to compensate imperfections after launch
  - Replaces massive structures with computers and actuators

# Principle of the wavefront control approach for NGST



## 1. COALIGNMENT AND COFOCUSING

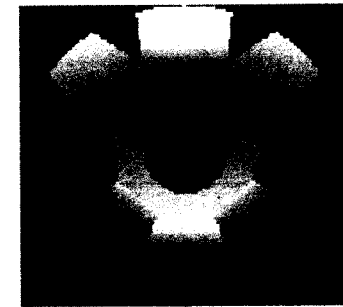
- Aligned to the accuracy of a single element telescope.
- Primary mirror piston  $\sim 5\lambda$  (10 microns) (limited by depth of focus of individual segment)



## 2. COARSE PHASING

Dispersed fringe sensing

$$\text{WF error} < \lambda$$

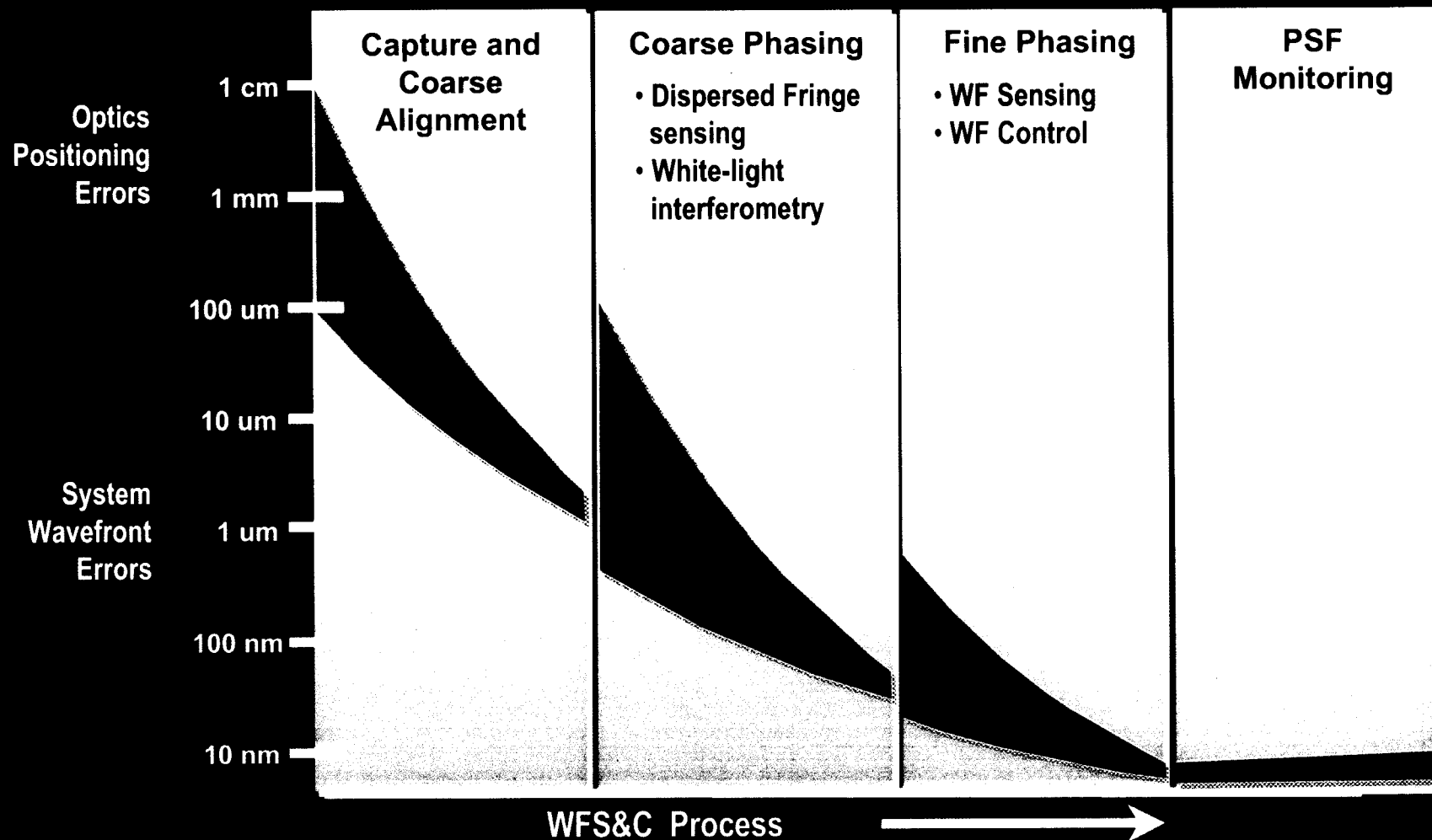


## 3. FINE PHASING

Phase retrieval

- WF measurement error  $< \lambda/100$
- WF control error  $< \lambda/20$

# Wavefront Improvement During WFS&C





# Modes and Algorithms

Government Baseline WFS&C System		Darkness	NIRCam	Other Cameras	Grisms (G)	Defocus Lenses (L)	Science Filters	Secondary Mirror Actuators	Rigid-body Actuators	Deforming Actuators	NGST Performance	Demonstrated (9)	TRL			
Control Mode	Algorithm										Capture Range (WFE)	Accuracy (rms WFE or WFSE)	Capture Range (WFE)	Accuracy (rms WFE or WFSE)		
Coarse Alignment	Segment ID	x	1				B		x	5	5 mm		5 mm		4	
	Capture	x	1				B		x	5						4
	Coarse Align	x	1				B		x	5			10 um	10 um		4
SM Align	WFS/Prescription Retrieval	x	1			x	N	x	x	5					3	
Segment Figure Correction	WFS/Prescription Retrieval	x	1,3,6			x	N				25 um / segment	<10 nm / segment			7	
	WFS/High Dynamic Range MGS	x	1,3,6			x	N				25 um / segment	<10 nm / segment			7	
	WFC									x		<100 nm / segment			4	
Coarse Phasing	Dispersed-Fringe Sensing	x	1,7	2			B		x	5	500 um	1 um piston error	500 um	100 nm piston error	4	
	White-Light Interferometry	x	1				B,M		x	5	20 um	100 nm piston error	20 um	100 nm piston error	4	
Fine Phasing	WFS/MGS	x	1,6			x	N				5 um	<10 nm	3 um	3.5 nm	7	
	WFC							x	x	x	5 um	<100 nm	3 um	20 nm	4	
Actuator Calibration	WFS/MGS	x	1,3,6			x	N	x	x	x		<10 nm		2 nm	4	
Camera-specific WFE Calibration	WFS/MGS			6			N					<10 nm		<10 nm	2	
PSF Monitoring	IPO/Prescription Retrieval	x	x				N					<10 nm		<10 nm	4	

- Notes:
1. Used in the unlikely event that the NIRCam is not available (contingency operations)
  2. 2 grisms/NIRCam channel; alternatively 1 grism/channel with different dispersion axes
  3. May prefer MIRI in the (unlikely) event that initial figure errors are very large (contingency operations, LMT configuration)
  4. 4 defocus lenses/NIRCam channel; alternatively 2 defocus lenses/channel with different offsets in each
  5. Rigid motion is provided using coordinated commands to deforming actuators in LMT configuration
  6. Secondary mirror will be moved to induce defocus in non-NIRCam channels
  7. Spectrometer channel used in dispersed-fringe mode (contingency operations)
  8. Fine Guidance System nominally active after Coarse Align is completed, though all modes can be performed without FGS (degraded performance mode for risk reduction)
  9. Demonstrated performance based on results from WCT-1, WCT-2, PRC and other platforms, generally in the visible

# Segment Mirror Phasing: Overview



## Product

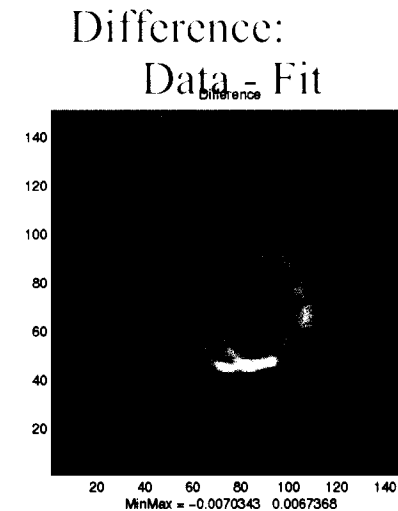
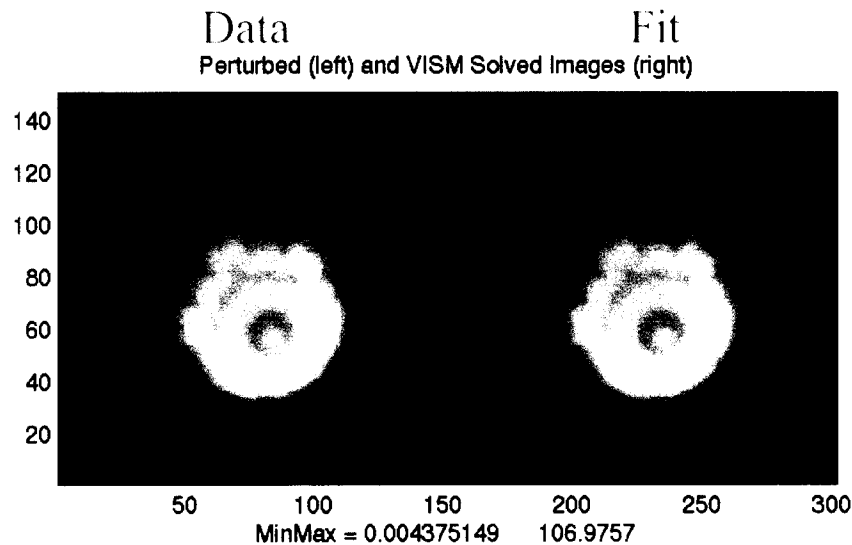
- Optical models: LM 7 Segment and Ball/TRW 37 Segment
- Secondary mirror alignment using VSIM
- Phasing segmented mirrors
  - Coarse alignment
  - Coarse phasing (DFS / WLI)
  - IPO
  - Fine phasing
- Influence effect: jitter, mirror aberration, etc ...

## Team

- F. Shi, D. Redding, P. Dumont, S. Basinger, J. Green, C. Ohara, S. Shaklan, and R. Baron

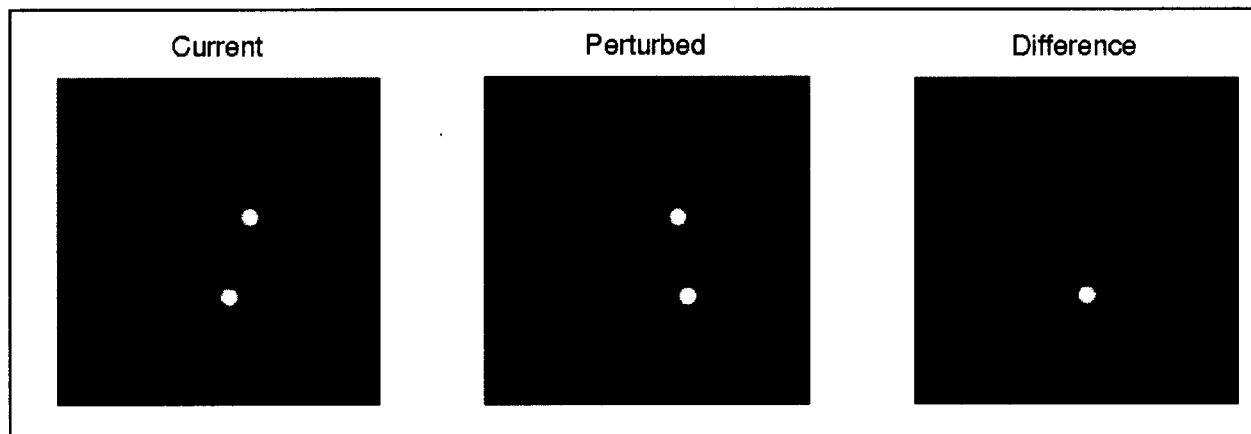
# Segment Mirror Phasing: VSIM by PJD

- Perturbations (6 dof) added to the Ball/TRW secondary mirror
- VSIM tries to fit the data image using the Levenberg-Marquardt least square solver
- All parameters are accurately retrieved except tilts which have larger errors
- On going work:
  - Tilts retrieval
  - Add noise
  - Add segment errors



# Methodology: Coarse Alignment - Tilt

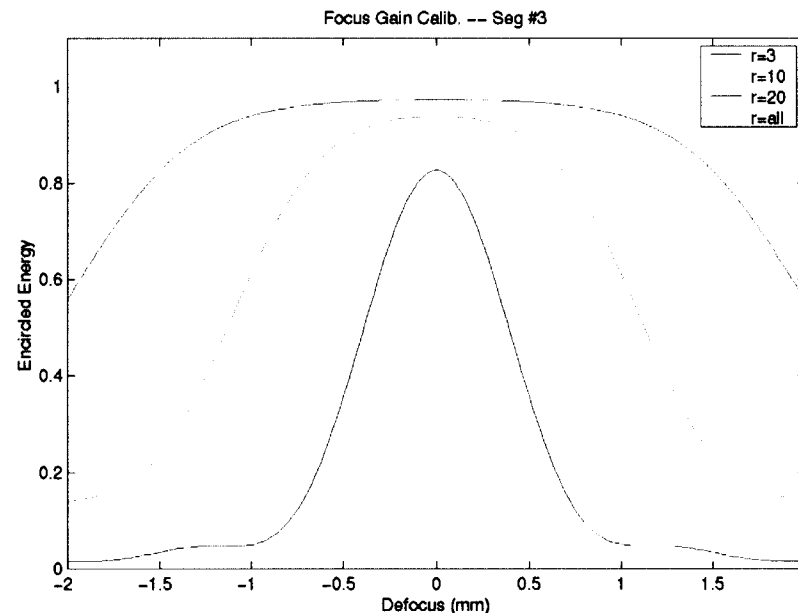
- Segment mirror identification, capture and co-alignment:
  - The tip-tilt position of a segment mirror is determined and corrected by the centroid of the spot formed by the segment mirror
  - The spot of segment mirror is identified and isolated by the image differentiation:  $\Delta I_i = \text{pos}|I_i(x_i, y_i) - I_i(x_i + \Delta x_i, y_i + \Delta y_i)|$ , where  $i$  is the  $i$ th segment and  $\Delta x_i$  and  $\Delta y_i$  are the known tilts given to the segment.
  - Perturbation tilts  $\Delta x_i$  and  $\Delta y_i$  can be program as as “encoder” to simultaneously identify multiple segment mirrors. They will also be used to guide the segment to “search and capture” the spot when the it is missing from the process of identification
  - With the knowledge of the guide star brightness a threshold will be used to determine if s spot from a segment mirror is missing



**Process of  
segment spot ID  
using image  
differentiation**

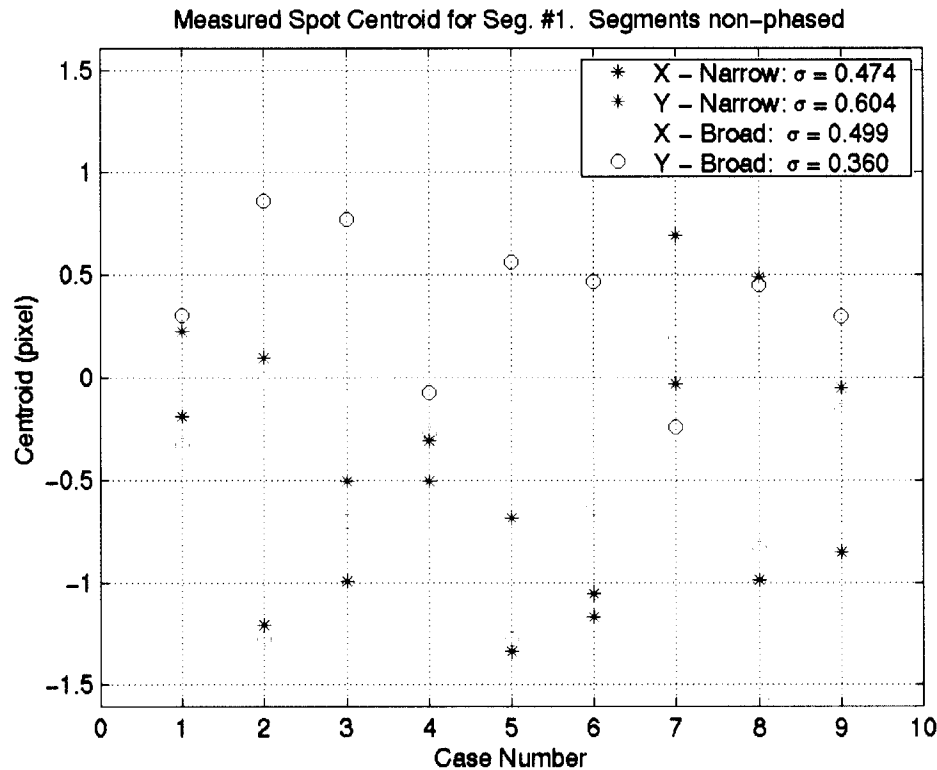
# Methodology: Coarse Alignment - Focus

- Segment mirror focusing:
  - A metric of “encircled energies at different radii” is used to guide the focusing process for each segment. The radius is determined accordingly to maximize the dynamic range of the metric as well as guarantee the sensitivity overlap between the metric. They are determined by modeling. Plot below shows a focus metrics for the WCT-2 model
  - When de-focus is large focus correction is calculated by geometric optics, a step which quickly focus the segment
  - When the de-focus is small a “hill-climbing” method is used
  - The focusing process stops when the depth-of-focus is reached



**Metric to focusing  
the segment mirrors**

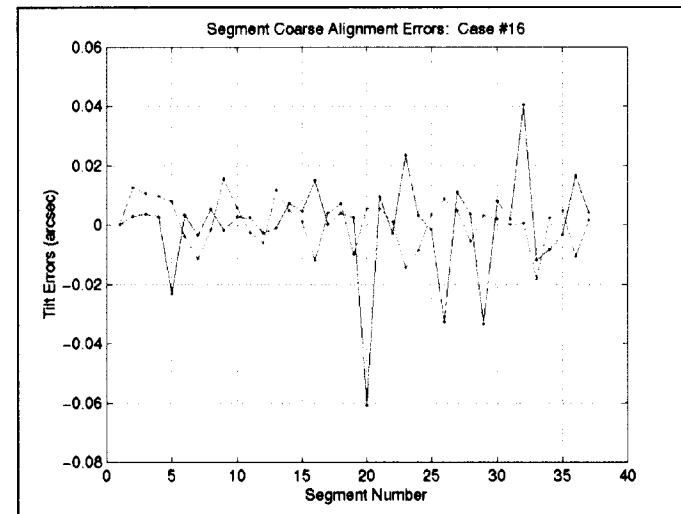
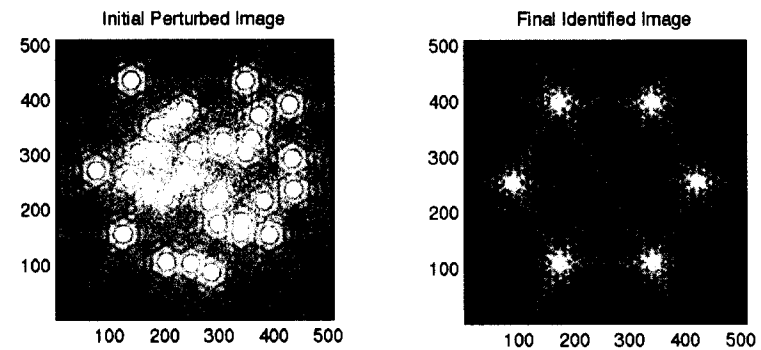
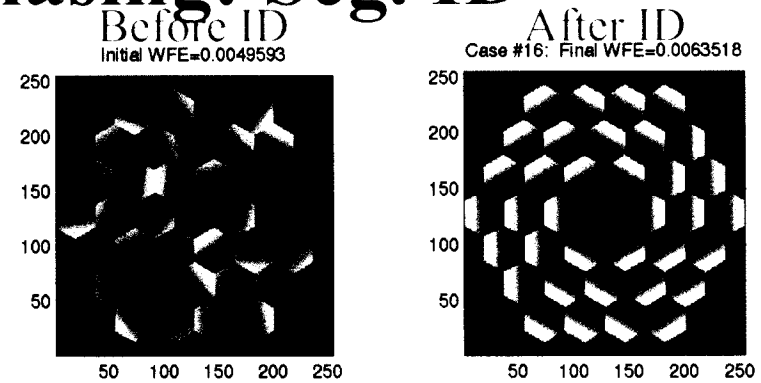
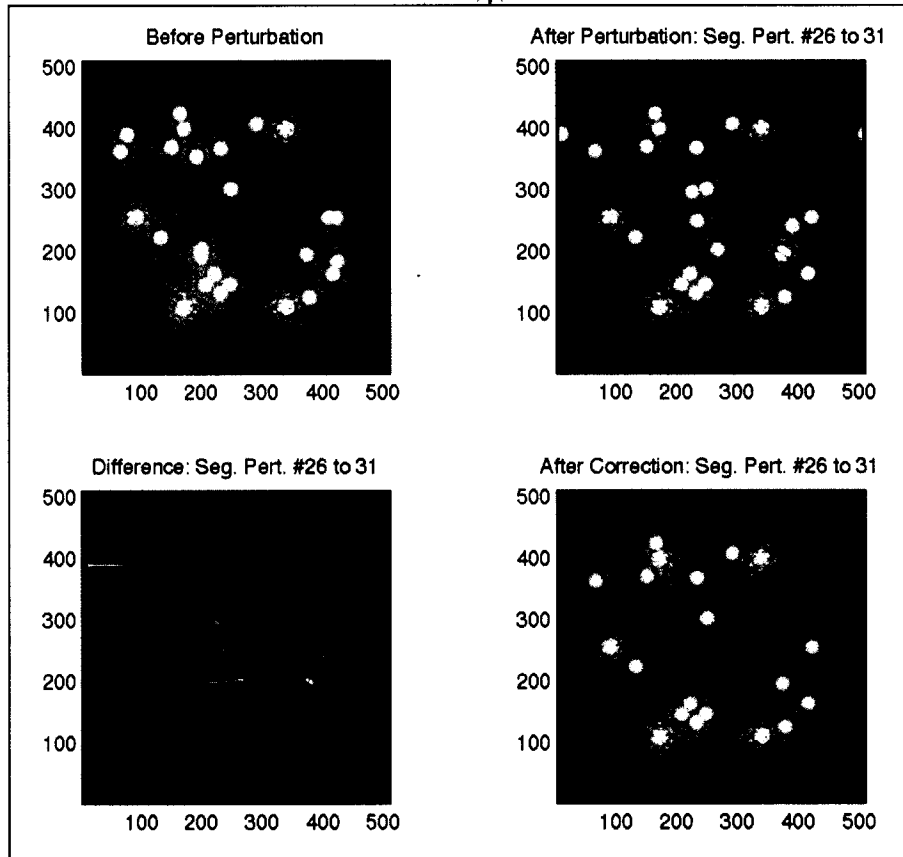
# Coarse Alignment: Centroid Accuracy and Wavelength Bandwidth



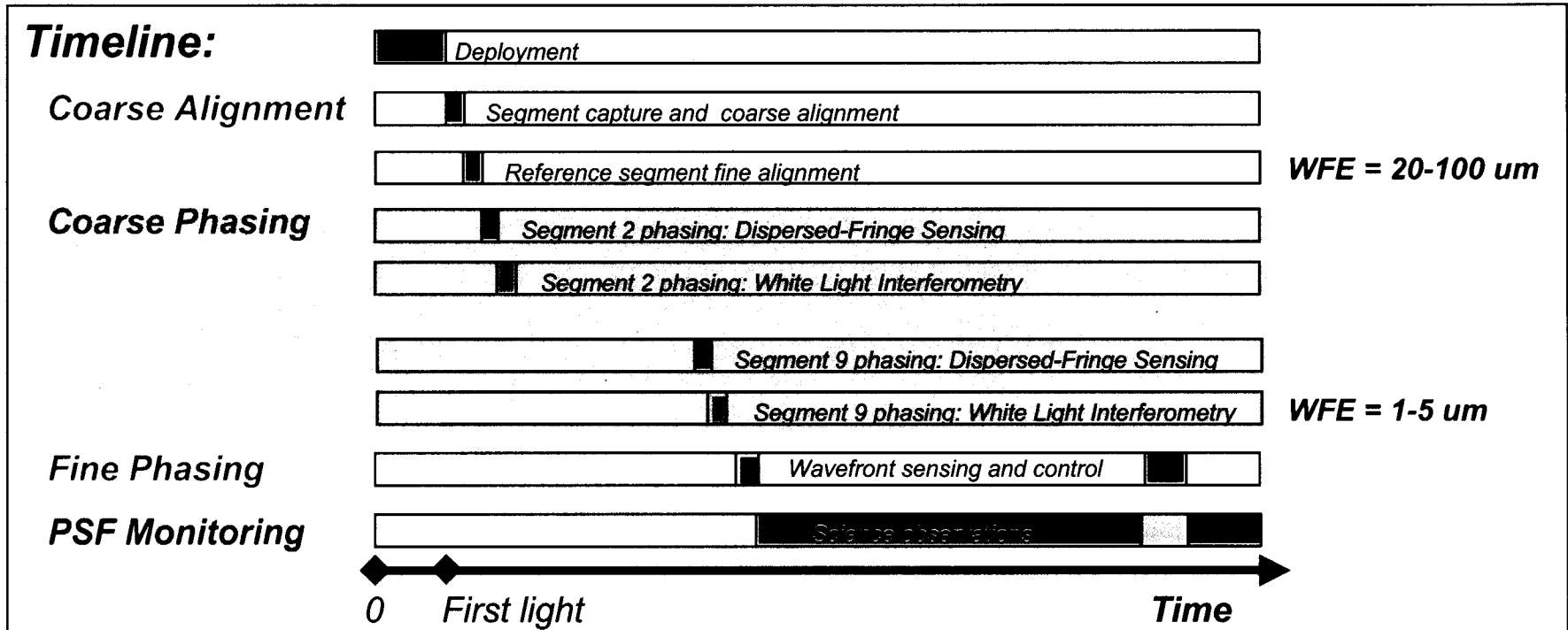
- WCT-2 experiment has shown that scattering of the segment spot centroid measurements are dominated by the lab seeing / jitter ( $\sigma \sim 0.5$  pixel). There is no obvious difference between using the images with the narrow band and broadband light source
- When the segment is not phased the differential image which used to calculation the segment spot centroid may contains fringes which may bias the accuracy of the centroid

# Segment Mirror Phasing: Seg. ID

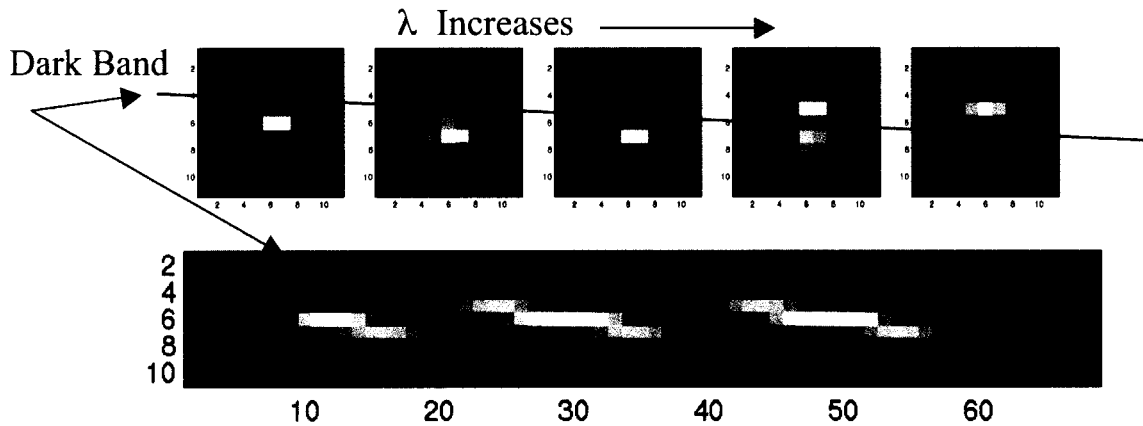
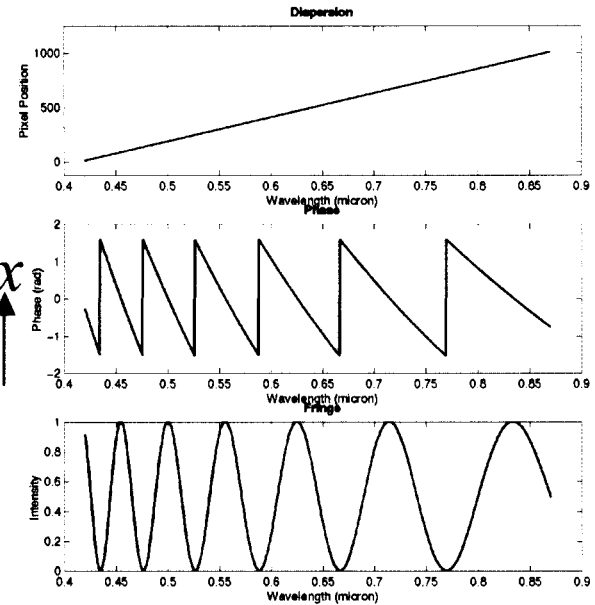
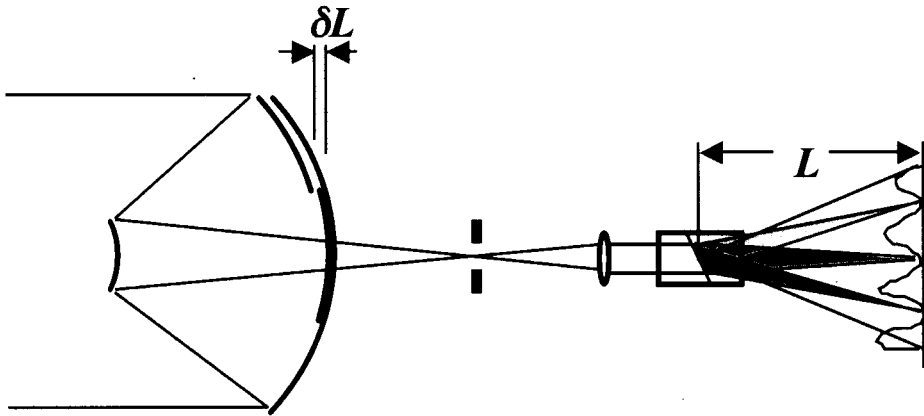
The process of segment Identification: 6 Seg.



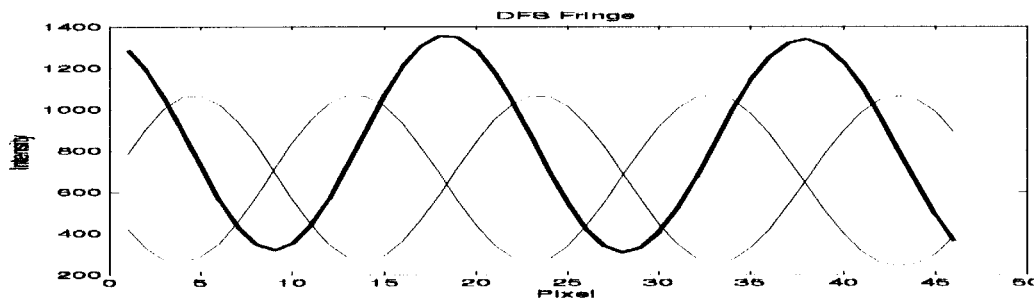
# Coarse Phasing



# Dispersed Fringe Sensor (DFS)



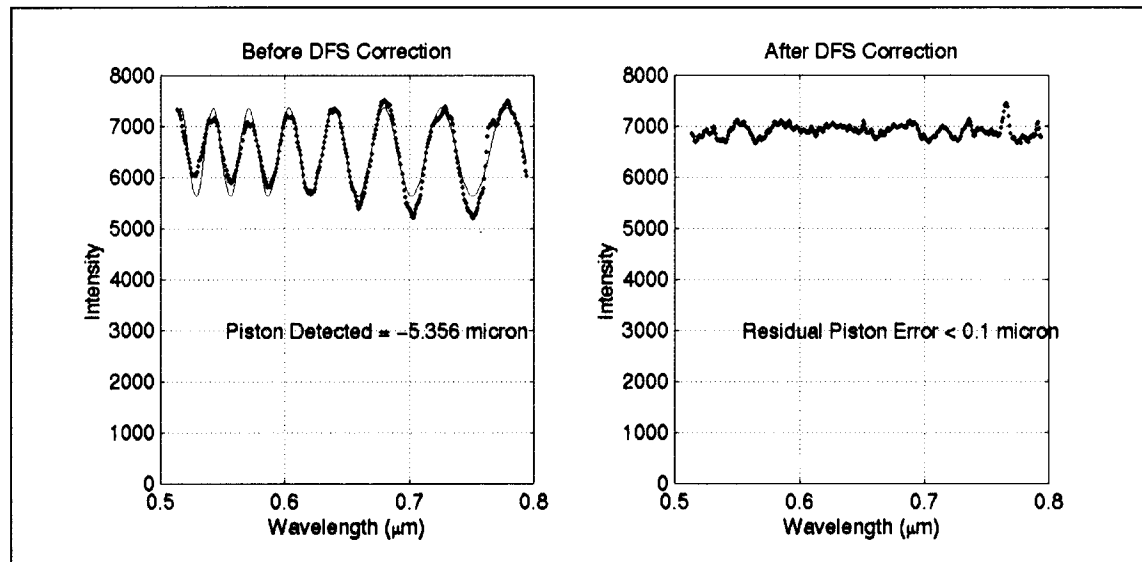
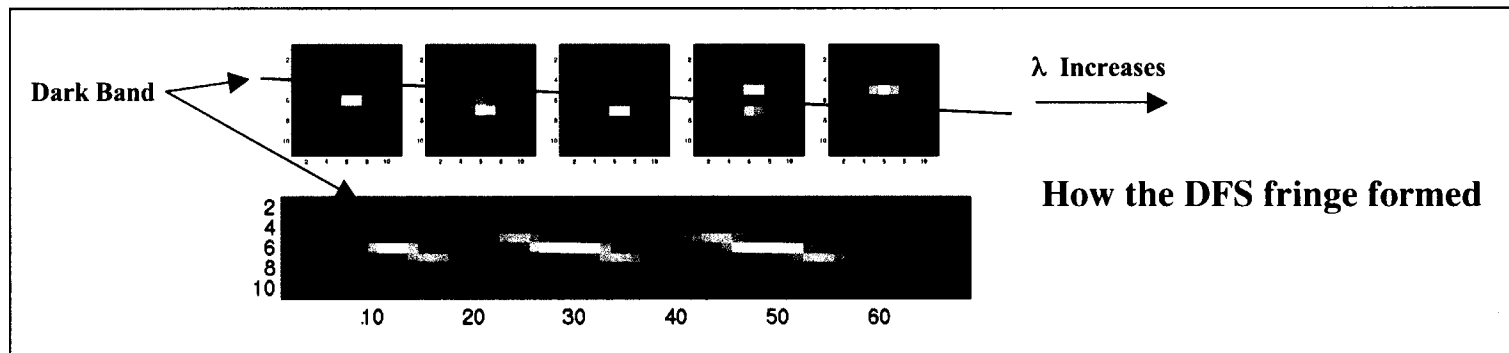
$x$



- DFS Modeled Fringe: DCATT Model
- Wavelength range:  $\lambda = 624.8 - 658.8$  nm
- Piston error:  $\delta L = 7$   $\mu$ m

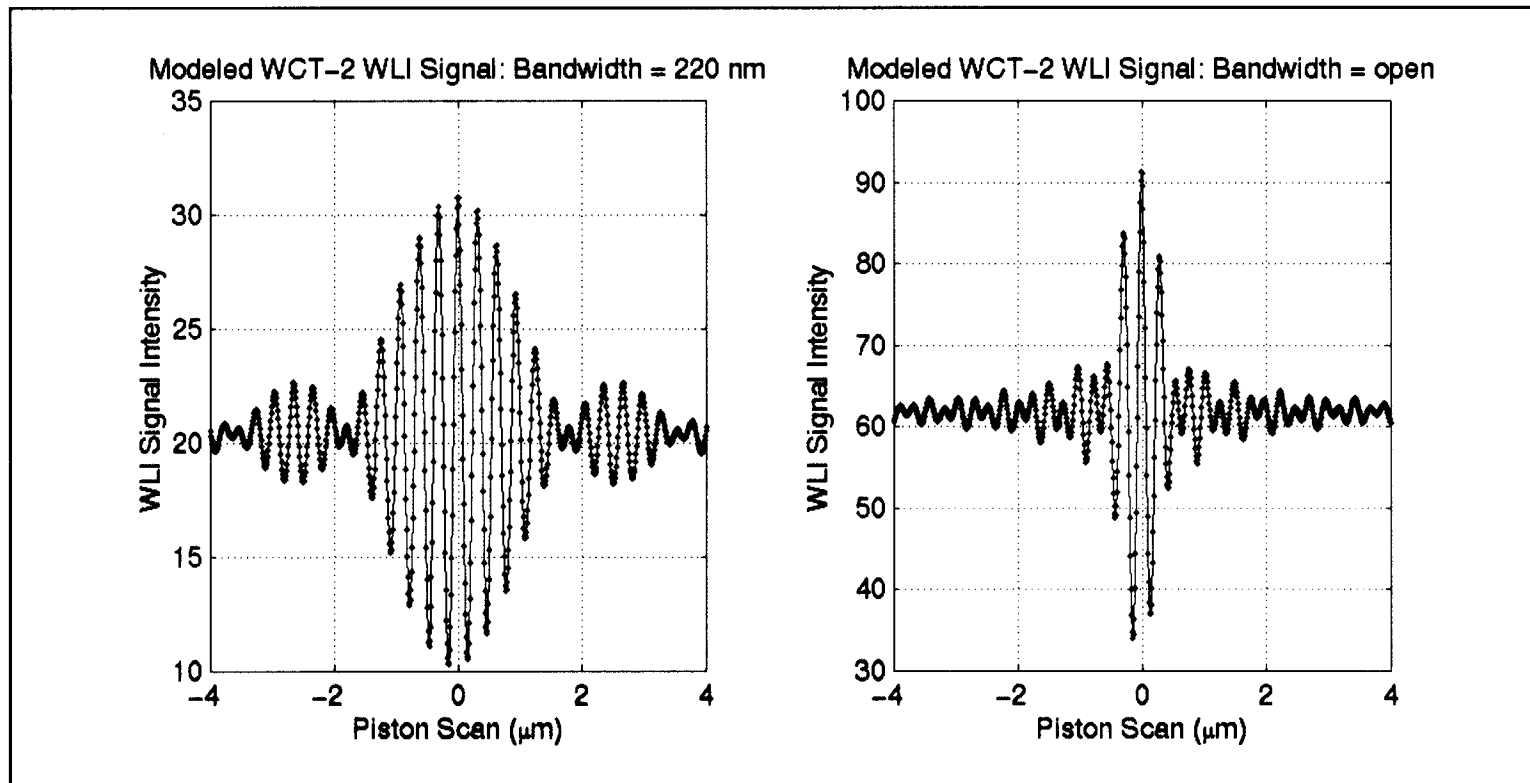
# Methodology: Coarse Phasing - DFS

- DFS detects the wavefront piston by fitting the modulated DFS fringe signals
- The period of the fringe depended on the amplitude of the wavefront piston error
- The orientation of the DFS fringes depended on the sign of the wavefront piston errors
- After correction ("*coarse phased*") the DFS fringe modulation disappears and fringe intensity is at the high level for all the wavelength - wavefront coherently added for all the wavelength, as shown in following WCT-2 test

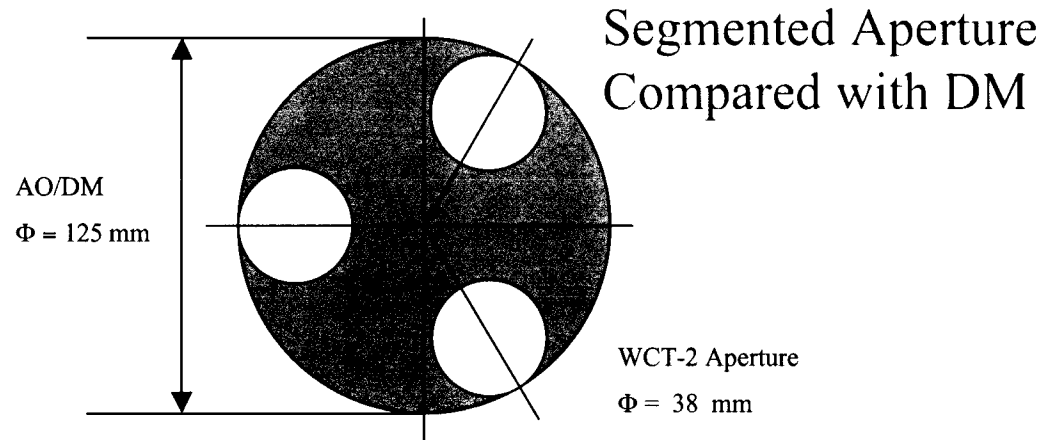
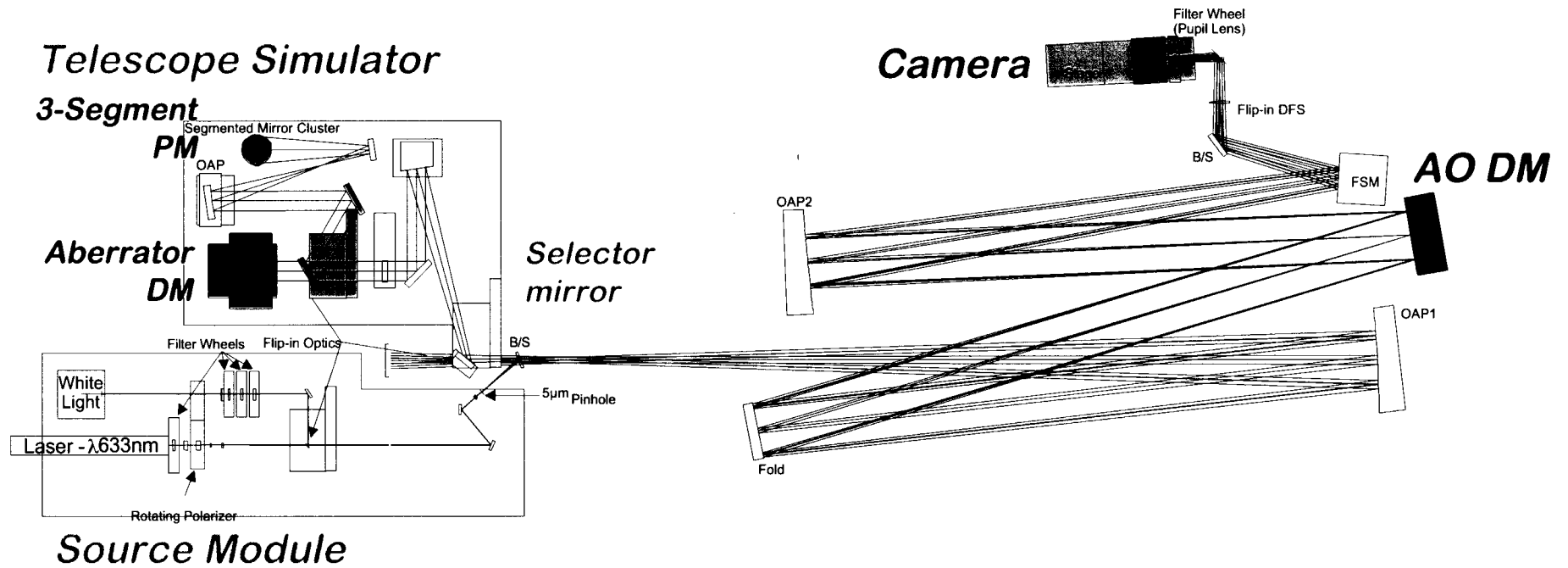


# Methodology: Coarse Phasing - WLI

- WLI signal is generated by taking a broadband PSF image at each piston scanning step and extract signal intensity in central sub-region of each PSF
- WLI detects the wavefront piston by using the correlation of the WLI signal with a reference (modeled) WLI signal
- The piston position which the correlation is maximum indicate the piston position at which the segment mirrors are phased
- The WLI method relies on the accuracy of the segment piston actuation and stability of the system
- Wavelength bandwidth determines the dynamic range of the WLI as well as the accuracy of the piston detection

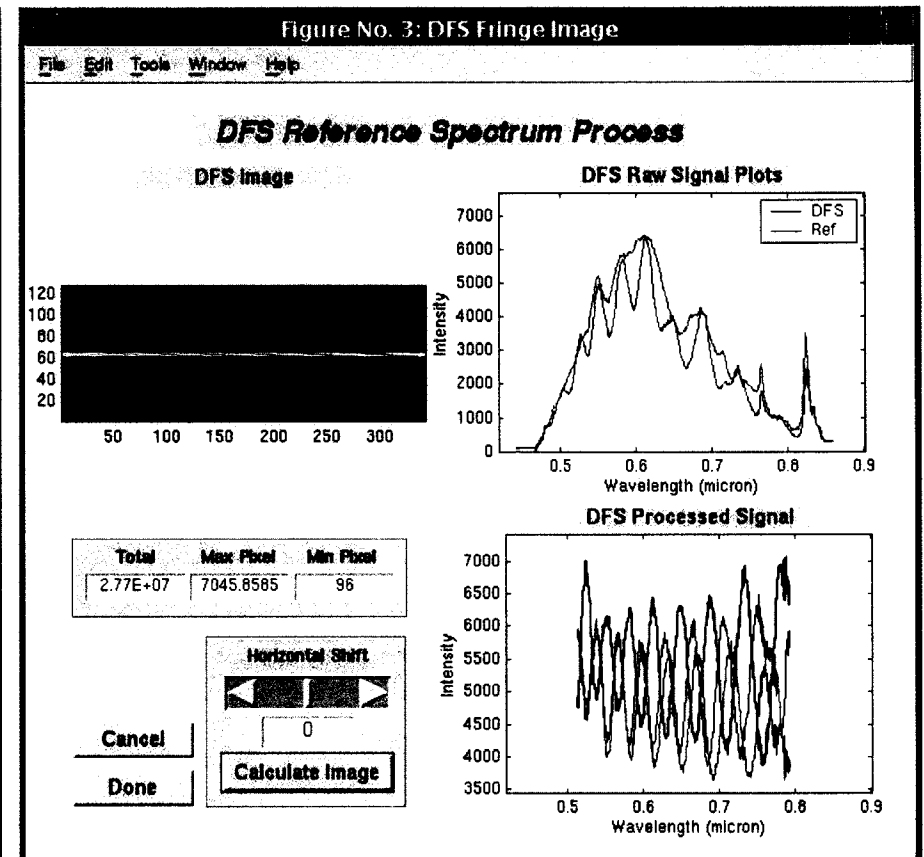
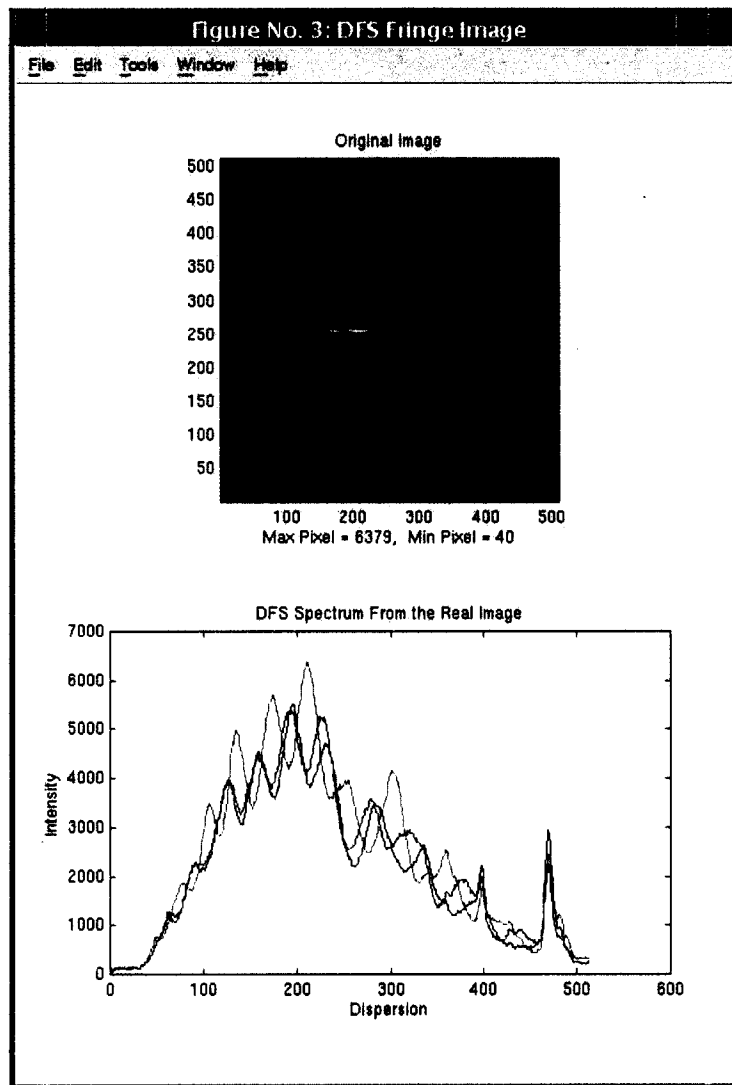


# WCT-2 Testbed Layout



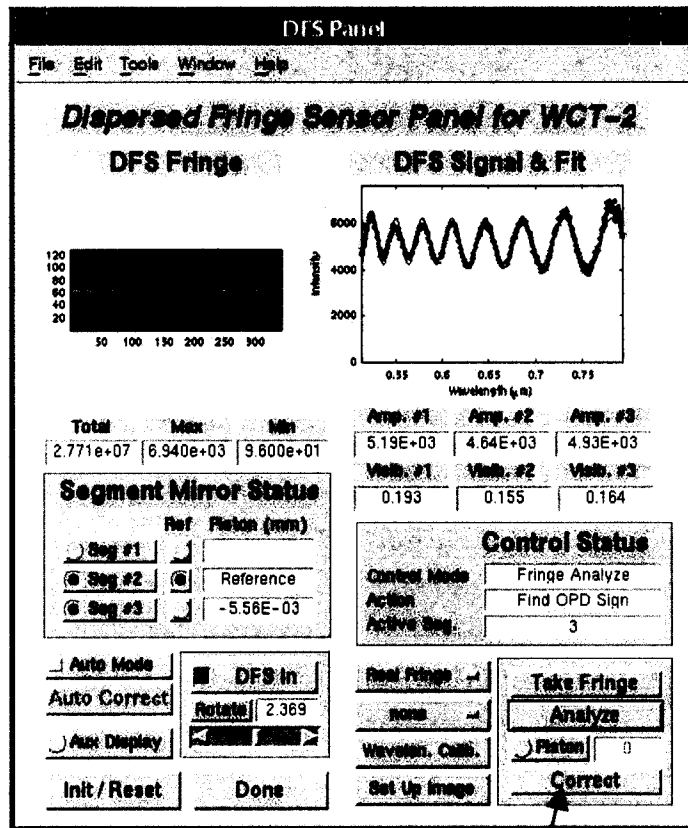


# WCT-2 Demo: Fringe Pre-Processing (Segs #2 & #3)



- Panels displayed during data taking
- Left panel shows the raw DFS image and signals
- Right panel shows the removal of lamp spectrum

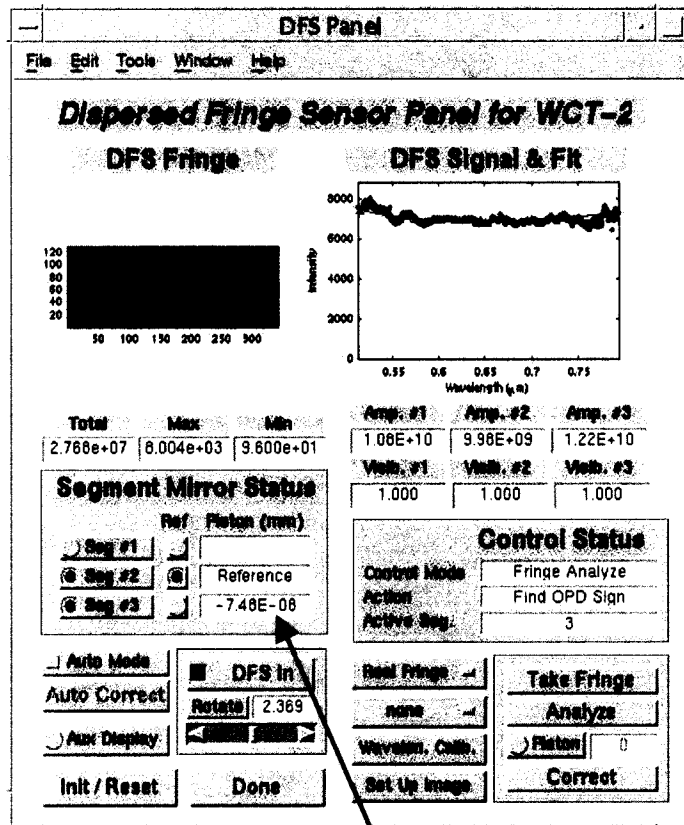
# WCT-2 Demo: DFS Analysis (Segs #2 & #3)



- Processed DFS image (Seg #1 tilted out)
- Processed DFS fringe from Seg #2 and #3 (dotted lines).
- DFS fitted curve (solid lines)
  - Fringe period determines piston magnitude
  - Relative phase between sidelobe traces determines the sign (up or down) of the piston
  - DFS analysis result:  
Relative Seg #3 Piston =  $-5.56 \mu\text{m}$

*Push here to implement piston correction*

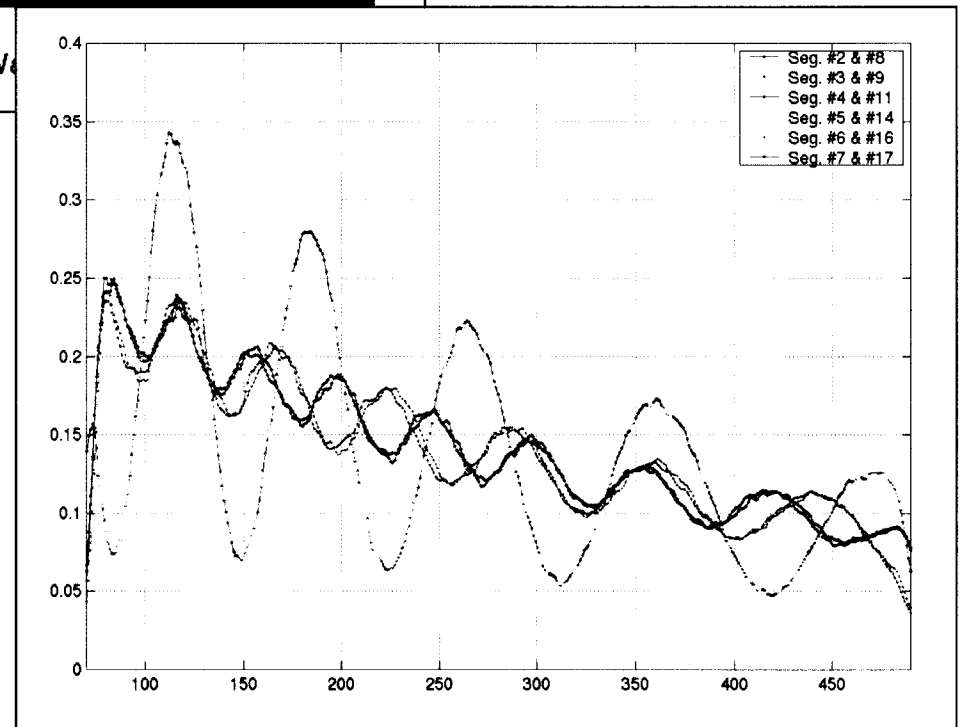
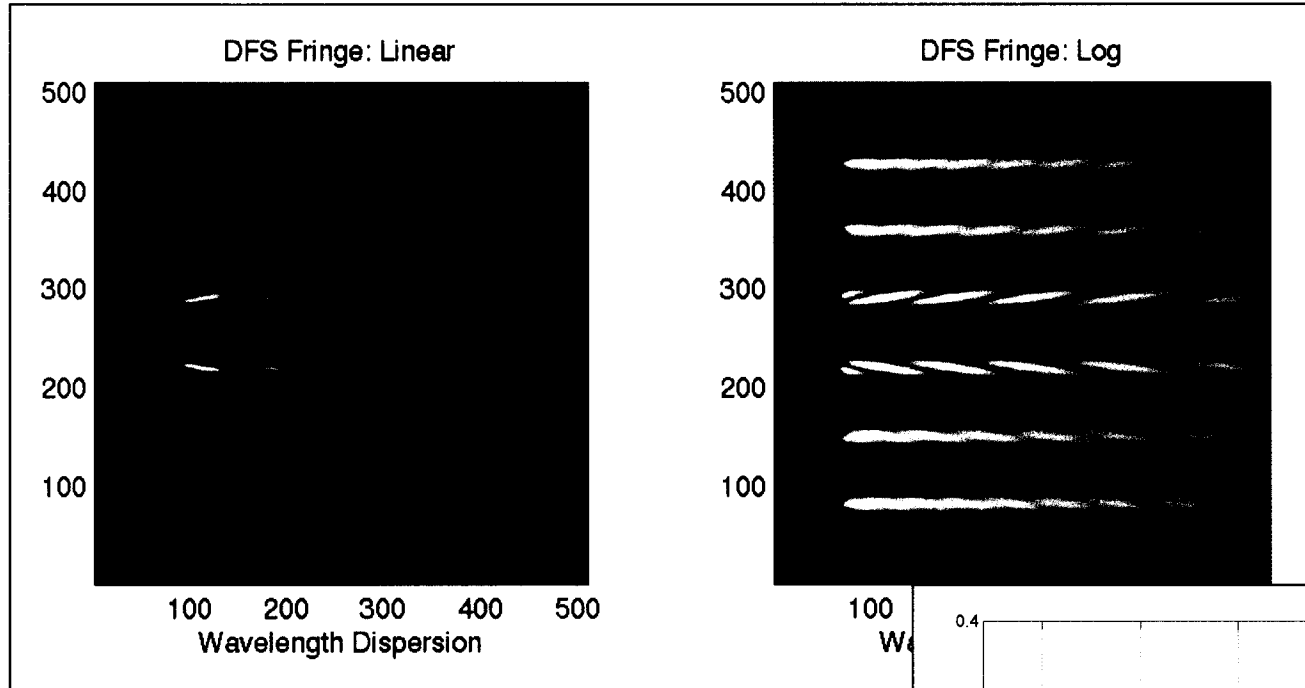
# WCT-2 Demo: After Correction (Segs #2 & #3)



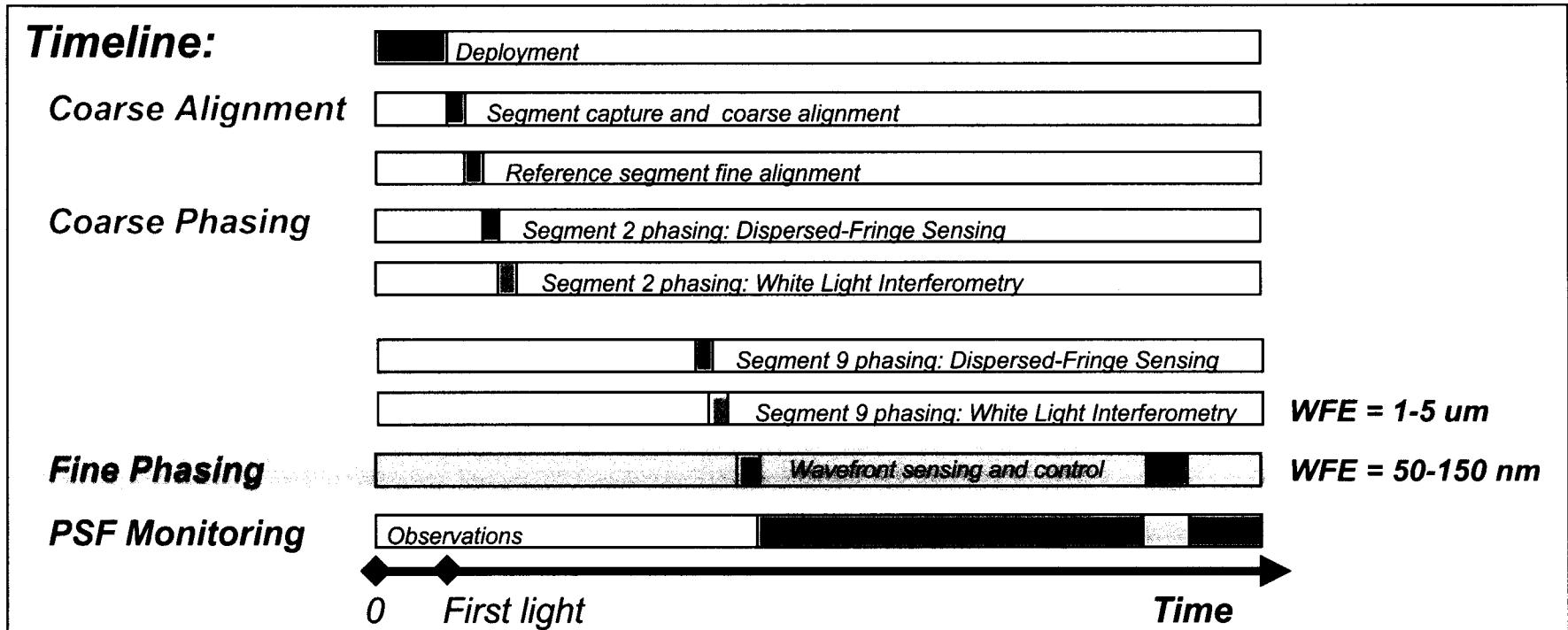
- Processed fringes after implementing correction show very little modulation
  - Modulation goes to 0 when segments are phased
  - Control has achieved sub- $\lambda$  residual piston error

*Detected piston reduced to near zero*

# Segment Mirror Phasing: Multi Center



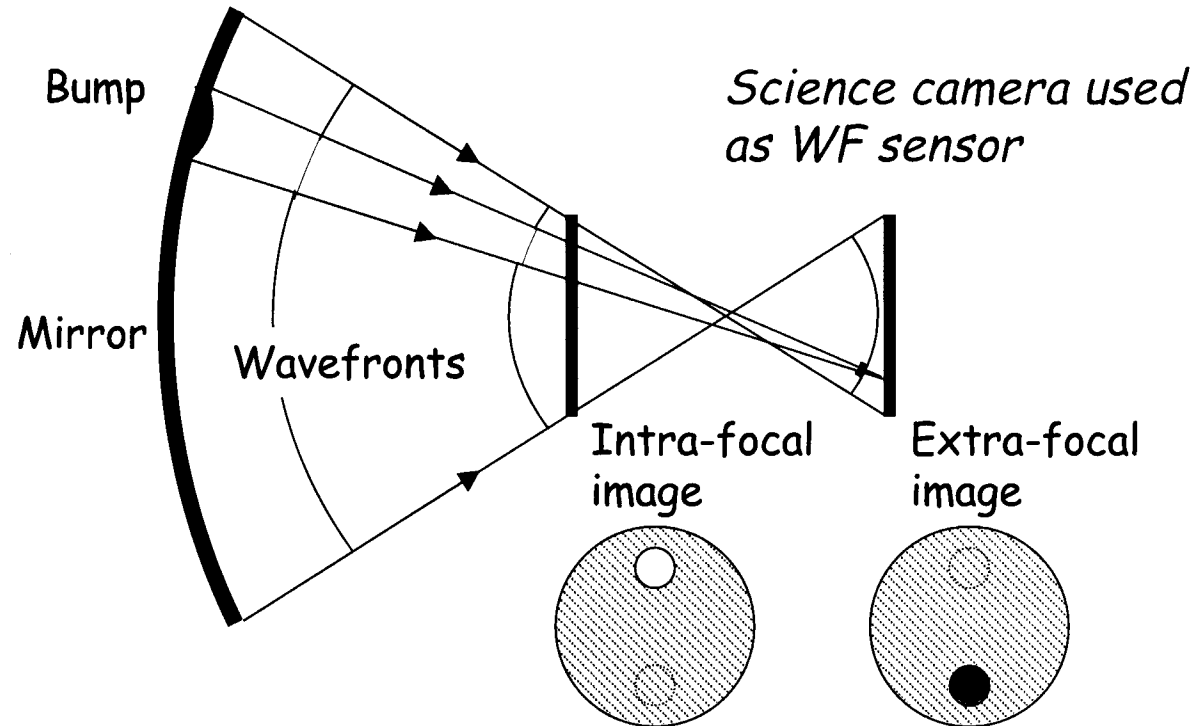
# Fine Phasing



# WFS Comparison

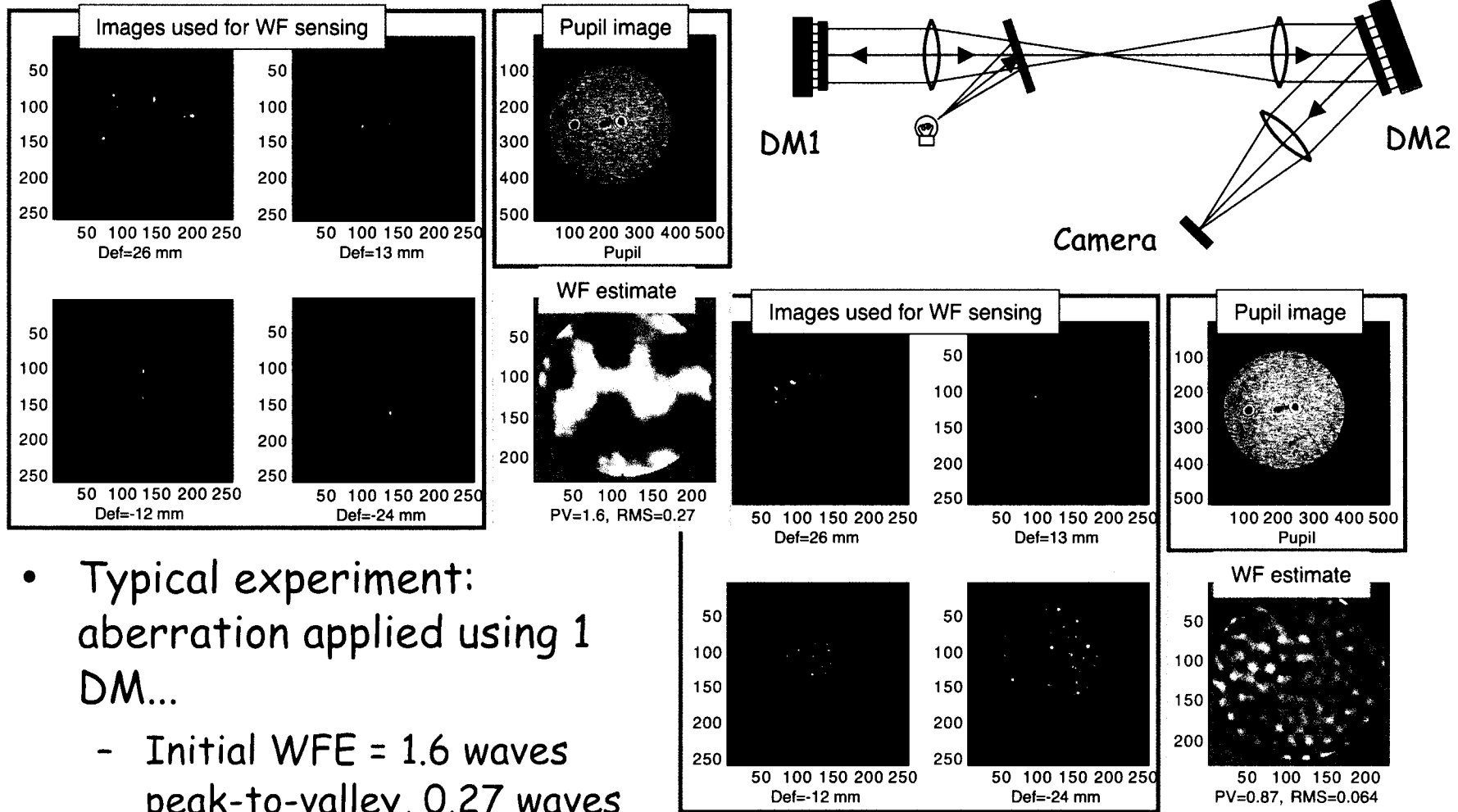
Method	Instrument	Common mode reject	Accuracy	Range	Spatial resolution	Noise & jitter	Resolves piston?
Phase retrieval	Any camera, any field	Yes	Excellent	Med (50 um)	High	Robust	Yes (multi-color)
Hartman sensor	Dedicated or flip-in	No	Good	High (1 mm)	Med	Robust	No
Shearing interf.	Dedicated	No	Good	Med	High	Robust	Maybe
Phase-shifting interf.	Dedicated	No	Excellent	Med	High	Sensitive	Yes (multi-color)

# WF Sensing Using Images



- A bump on the mirror surface shifts the focus of a patch of the beam
- This shows up as a bright spot on one side of focus and a dark spot on the other
- Computer processing of multiple defocussed images correlates the intensity variations in each, derives common WF phase map
- This phase map is then used to compute new control settings

# Example from NGST WFC Testbed

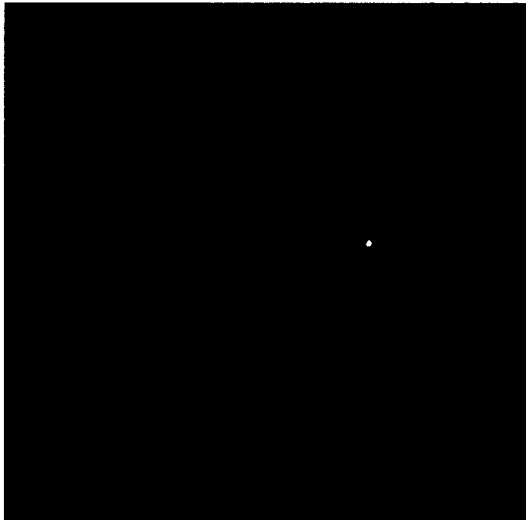


- Typical experiment: aberration applied using 1 DM...
  - Initial WFE = 1.6 waves peak-to-valley, 0.27 waves RMS

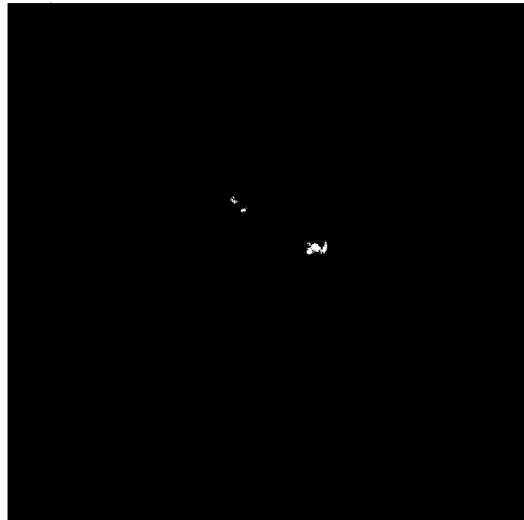
- ... and corrected using second DM
  - After control WFE = 0.87 waves PV, 0.064 waves RMS

# WCT-2 Five-Image Phase Retrieval

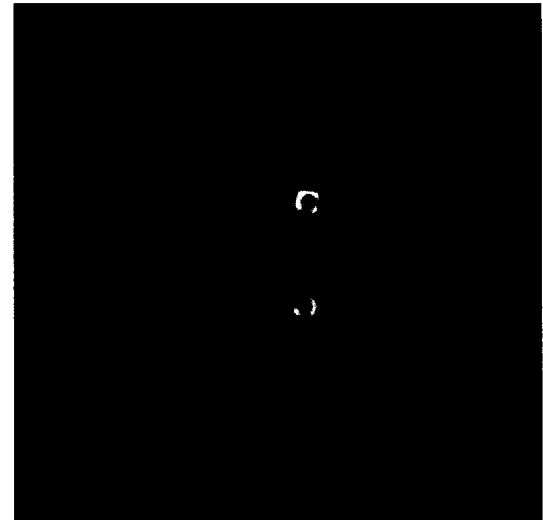
defocus = 25 mm



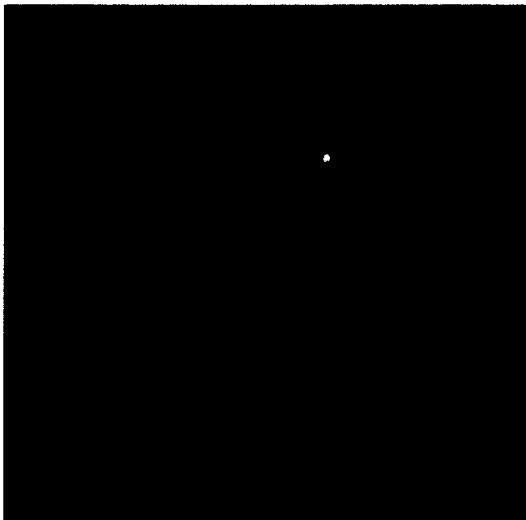
defocus = 12.5 mm



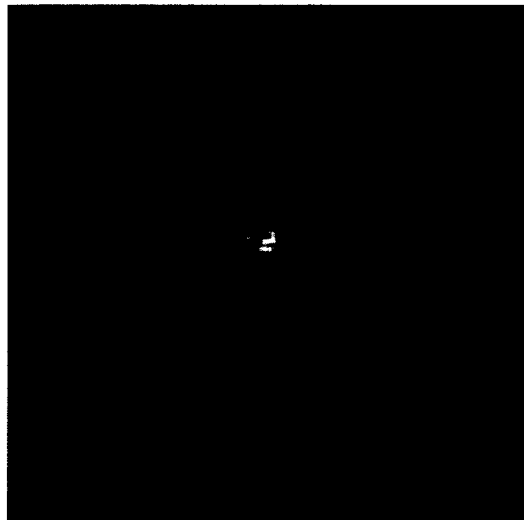
defocus = -12.5 mm



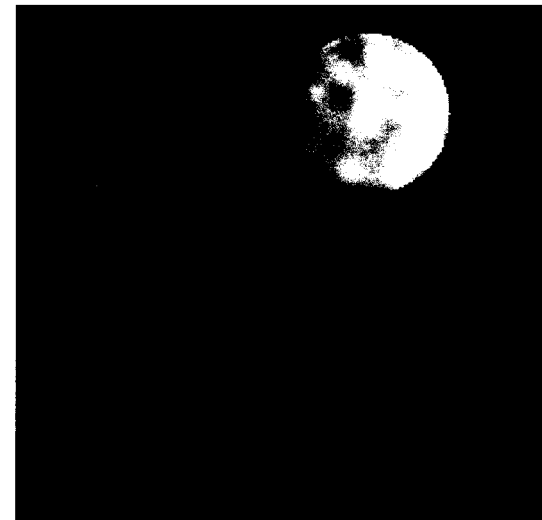
defocus = -25 mm



defocus = 0.8 mm



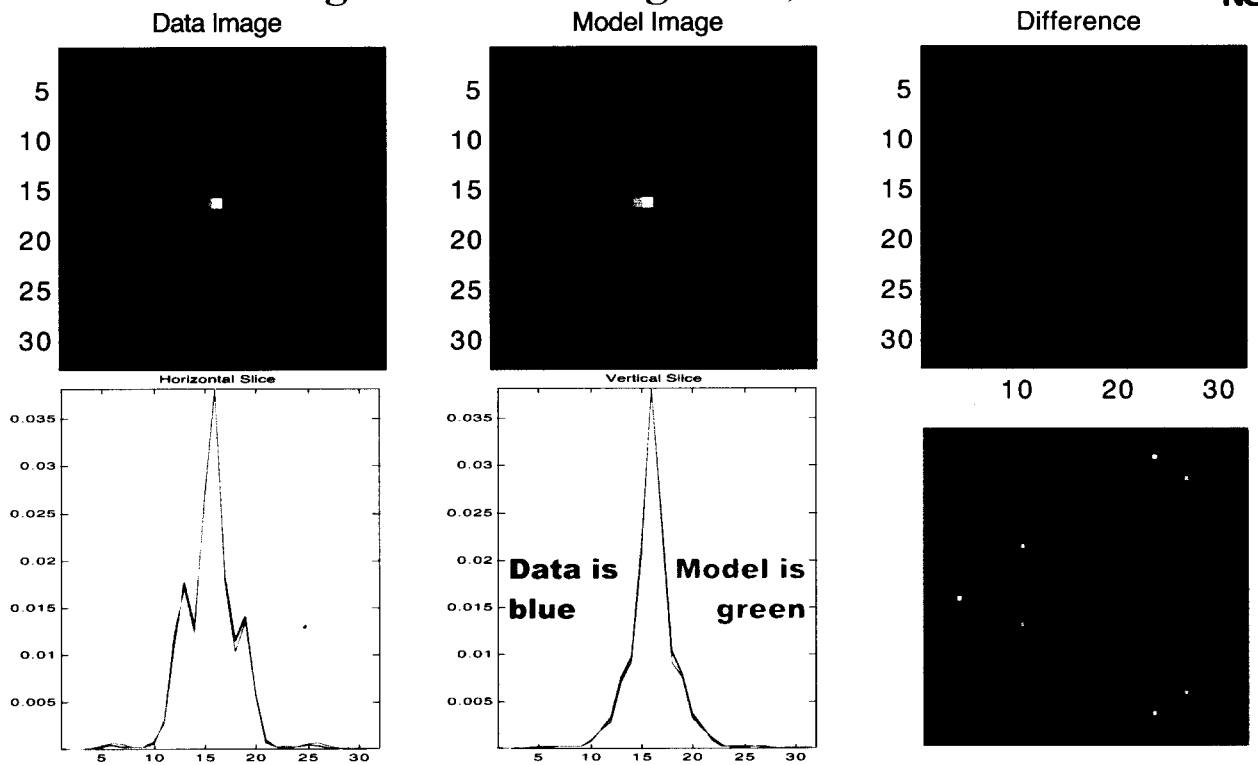
estimate



RMS = 0.237 waves

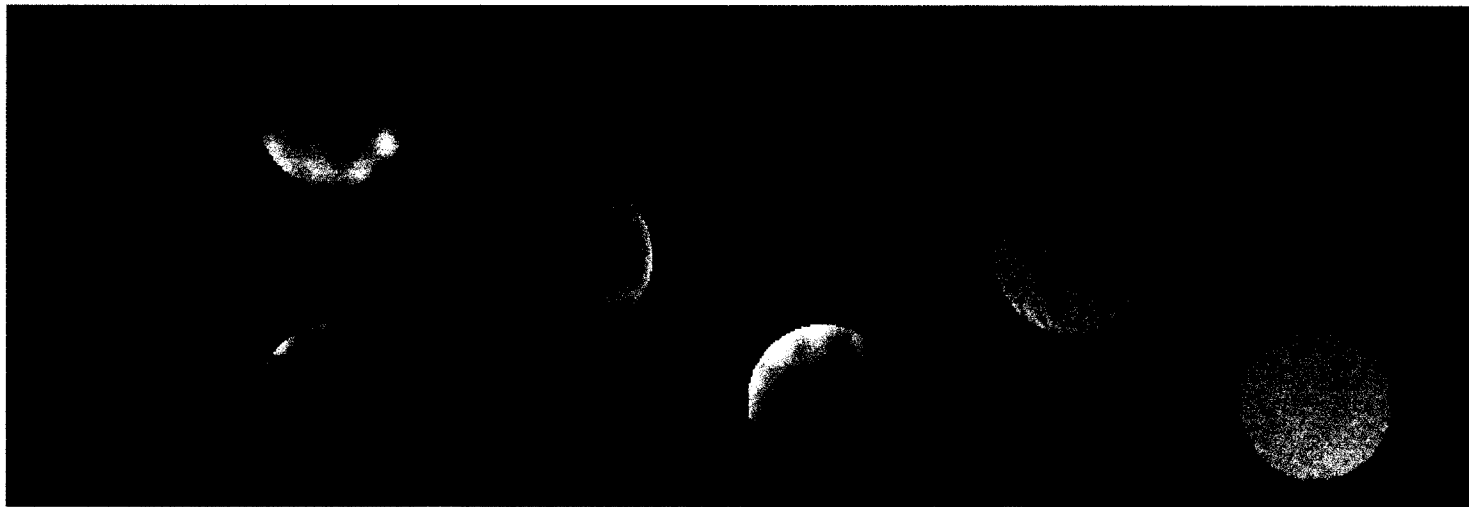
P-V = 1.11 waves

# Infocus Image: No PSF Magnifier, $\lambda = 900$ nm



- WCT-2 data
  - 900 nm filter
  - 0.1 sec exposure time for min jitter
  - 250 frames
  - Subpixel shift-and-add
  - Frame selection
  - No PSF magnifier
  - Blur half-width = 0.54 pixels
  - Match = 0.026 RSS vs. total of 25

# WCT-2 Phase Retrieval: Segment Piston



initial

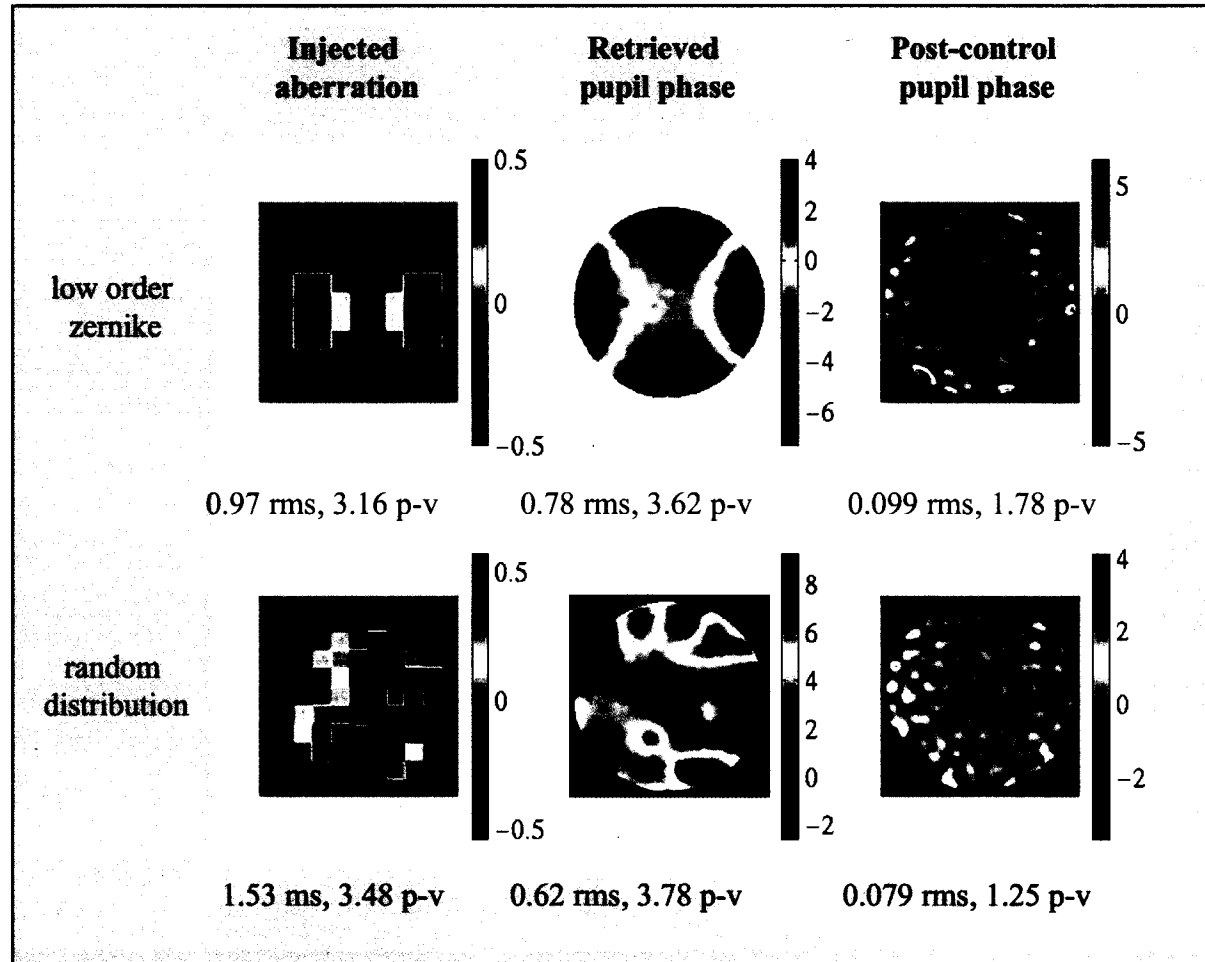
piston segment 3

difference

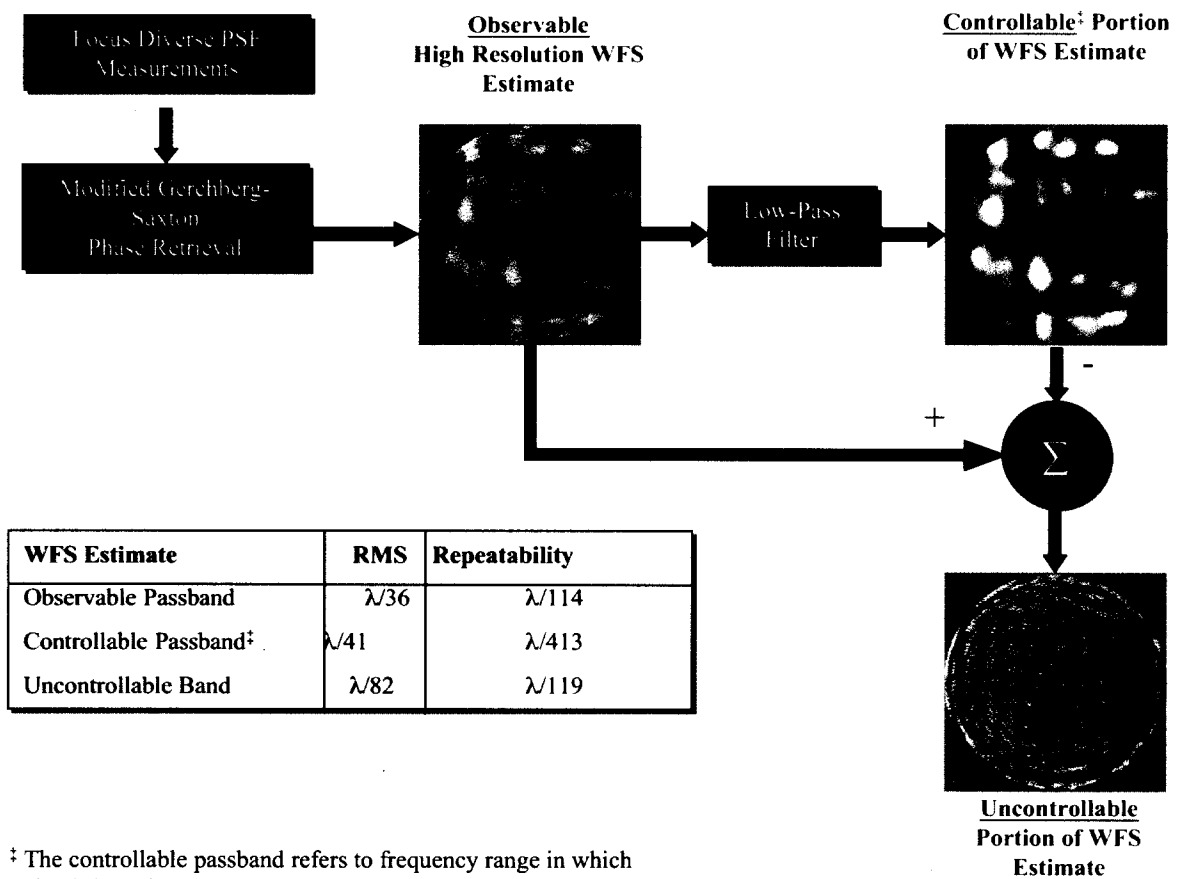
# High Dynamic Range Feedback Phase Retrieval & Wavefront Control



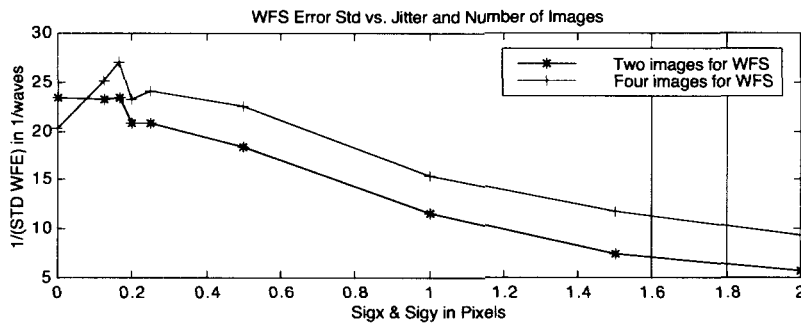
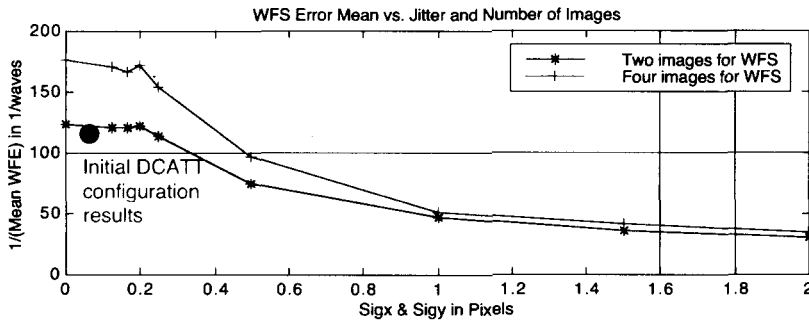
- WCT-1 Testbed Results
- High aberration injected at testbed SMDM
- Phase retrieved & unwrapped at 632.8 nm
- Phase controlled at testbed AODM



# Spatial Frequency Content of a WFS Estimate



# WFS Insensitive to Jitter



Monte Carlo simulation, 100 trials/pt

DCATT optics

Double-pass telescope

Random misalignment

WFE < 1 wave for each case

15 DN read noise

12 bits dynamic range

Phase retrieval parameters

$\lambda = 632.8 \text{ nm}$

2x oversampled

Two images:

Defocus =  $\pm 15 \text{ mm}$

Four images:

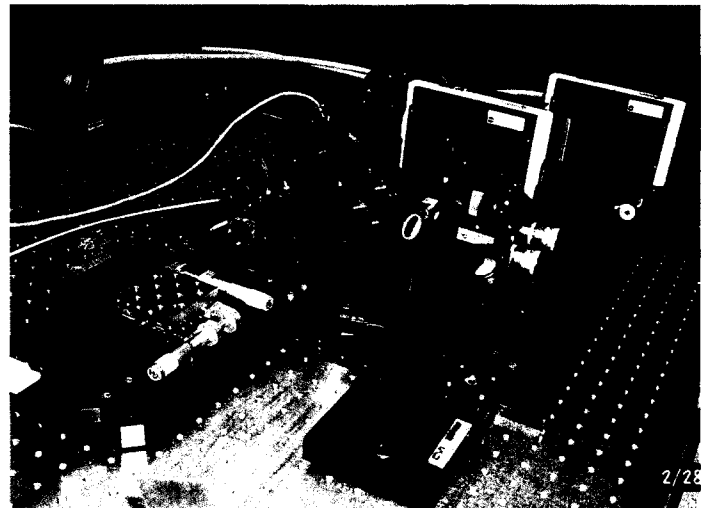
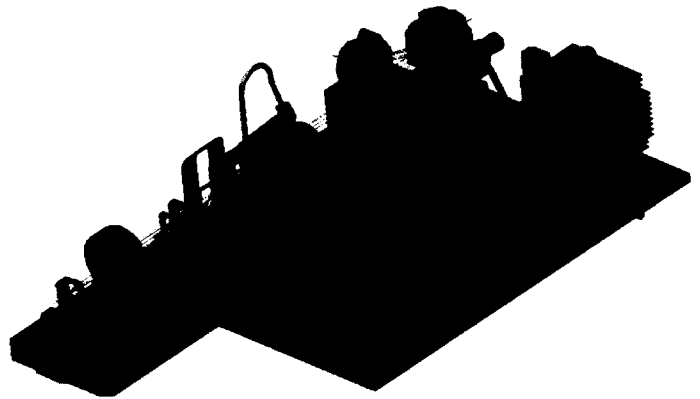
Defocus =  $\pm 15, \pm 7.5 \text{ mm}$

2 images run to full well

- Modeling results indicate good performance possible even with significant jitter
- Born out by results using WCT
  - Data at 0.1 pixel jitter
  - Reliable WFS in high jitter cases (0.4 pixel)

## NGST Phase Retrieval Camera

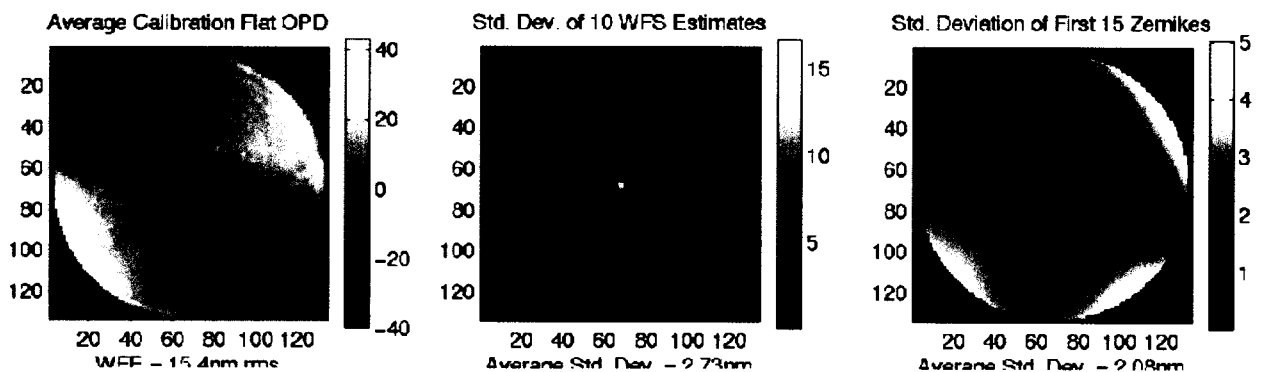
- The Phase Retrieval Camera (PRC) is a portable, self-contained *image-based wavefront sensing device*
- Enables wavefront control experiments anywhere there are appropriate optics for testing
  - Large lightweight PM segments in cryo-vac test facility (AMSD)
  - Deformable mirror testing
  - NGST engineering test optics
  - NGST primary optics





## PRC Calibration Repeatability

- With the calibration flat in place, 10 sets of WFS measurements were taken in air over a 2 hour time span.
- The mean OPD shown below on the left, shows alignment errors in the PRC consisting mainly of astigmatism. The overall WFE of the system is 15.4nm rms wavefront ( $\lambda/44$ ). (More recent alignments show 8 nm error.)
- The standard deviation of the OPD computed from the set of 10 estimates shows a small level of WFE variation that occurs mainly in the lower order aberrations.
  - The variations of the low order aberrations was on the order of 2.08nm rms wavefront ( $\lambda/325$ ).
  - The overall standard deviation of the WFE had an average of 2.73nm ( $\lambda/247$ ).



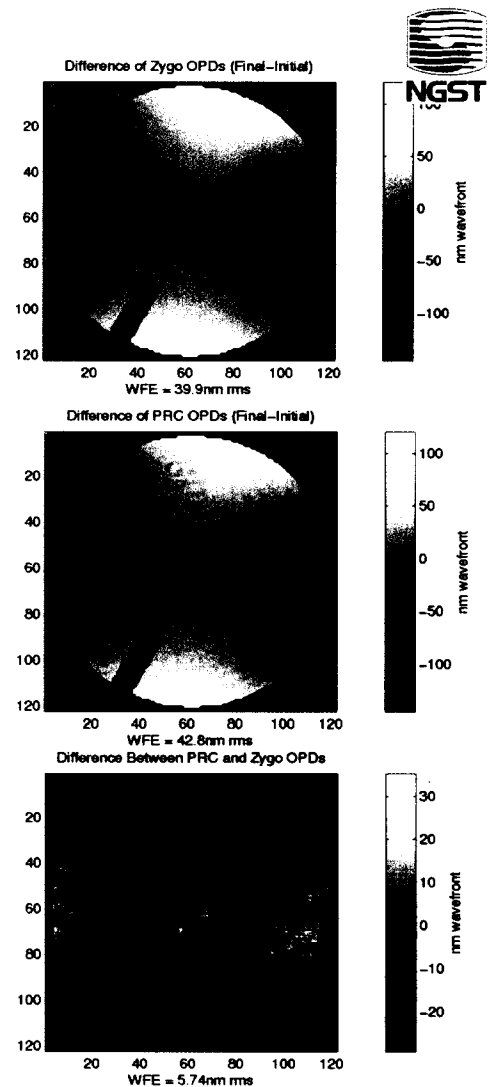


## PRC-Zygo Small Optics Test

- Test uses a single small  $\lambda/10$  spherical mirror equipped with a deformation-inducing screw
  - Fiducial plate constrains aperture, registers orientation between PRC and Zygo
  - Test requires moving the mirror between PRC and Zygo test stands
  - Nylon set screw induces variable levels of astigmatism
- Experiment compares *differential measurements* to compensate non-common mode errors between PRC and Zygo
  - Observed drift in deformation, assumed due to use of nylon screw
  - Control experiment showed good repeatability for relaxed mirror

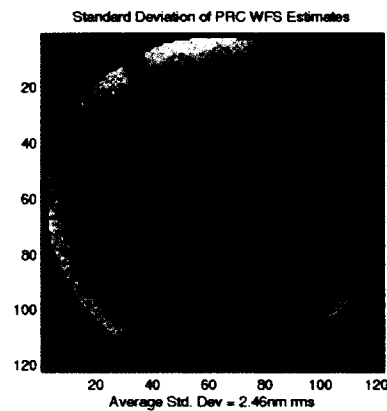
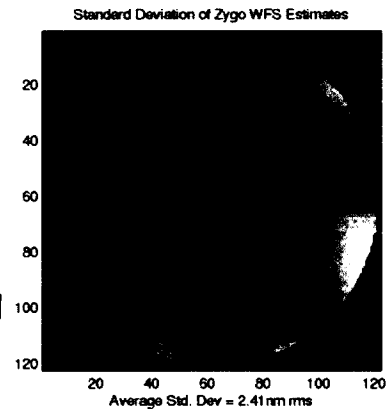
## Set Screw Influence Comparison

- This OPD represents the set screw influence function that was measured by the ZYGO. The dominant mode of this OPD is astigmatism.
- The influence estimated by the PRC is very similar to the ZYGO result. The most notable difference is a faint "ringing," due to SNR variation in the defocussed image set. This effect can be reduced by defocus selection and spatial-frequency weighting in MGS outer-loop averaging.
- The difference of the influence functions is on the order of 5.7nm rms. This error is fairly broadband. (4.1nm in first 45 Zernikes)

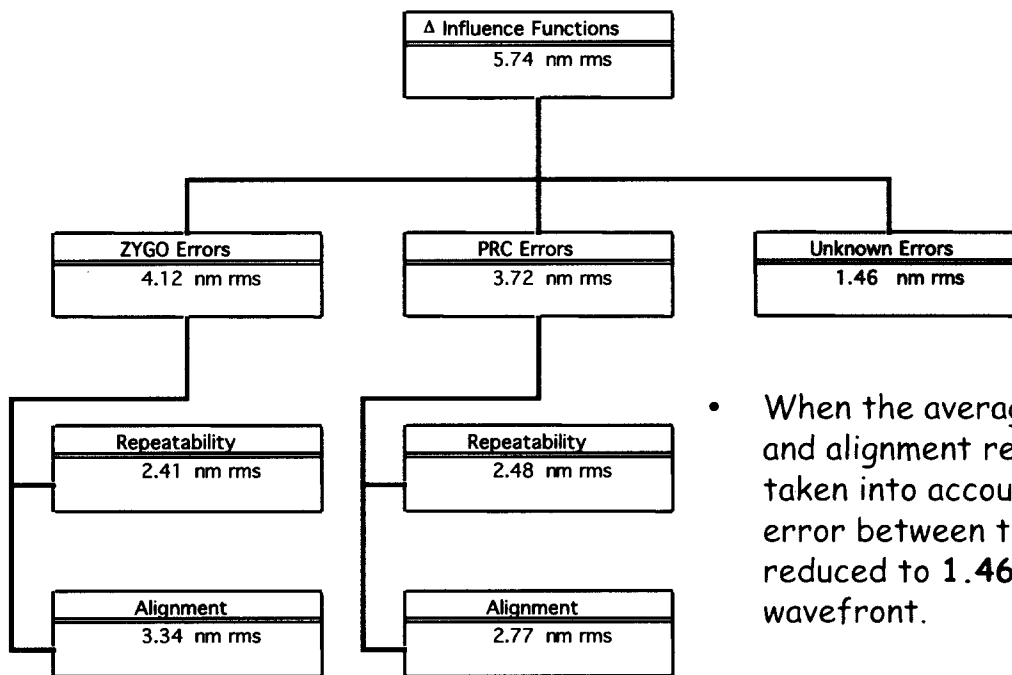


# WFS Estimate Repeatability

- Additional measurements were taken to help partition the measurement repeatability from the other dynamic aberrations.
- Here, the standard deviation is computed on a point-by-point basis through the set of WFS results that were taken *without realigning the test optic*.
- While the ZYGO (top) and the PRC (bottom) both demonstrated similar levels of WFS repeatability, the distribution of this repeatability was quite different
  - The ZYGO repeatability errors are dominated by dynamic low order aberrations
  - The PRC repeatability appears more broadband

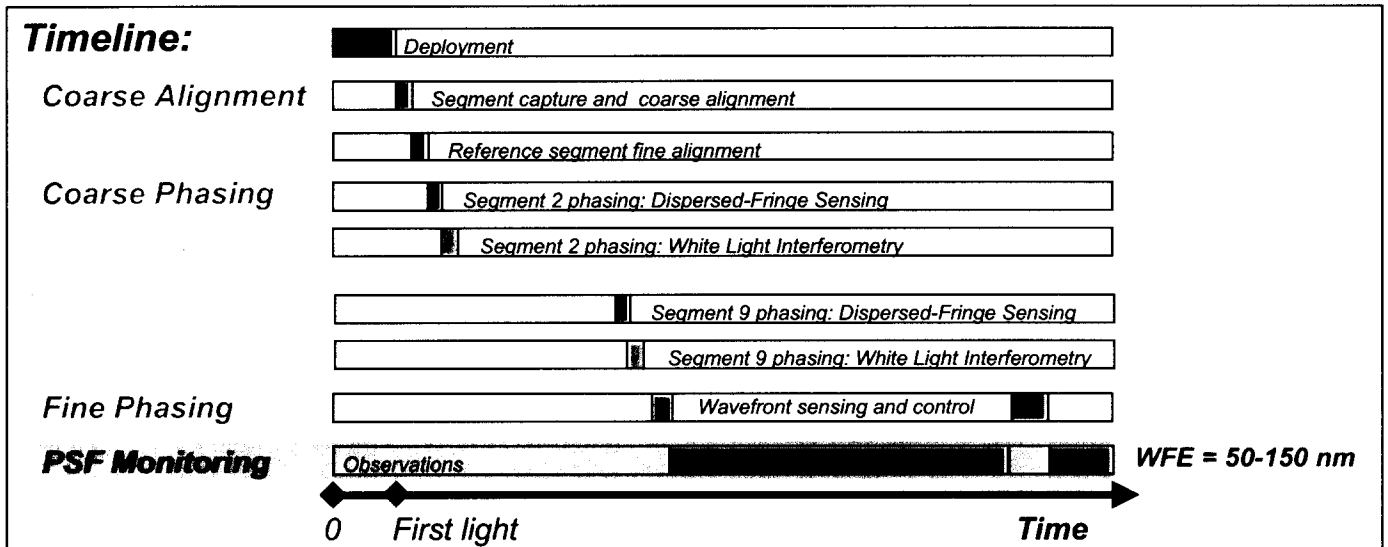


# WFS Error Budget for Experiment

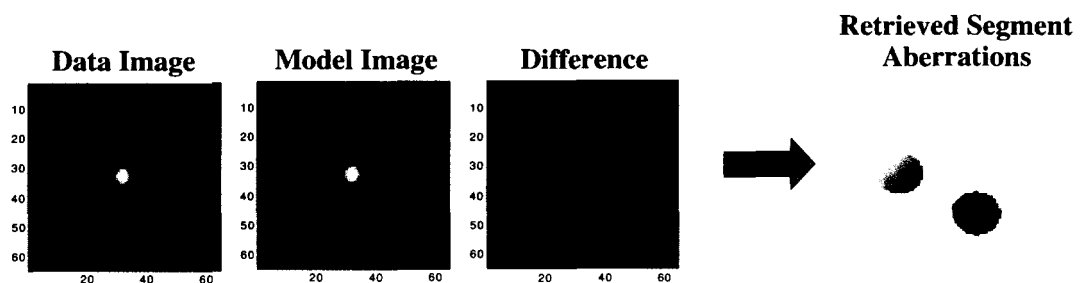


- When the average measurement and alignment repeatabilities are taken into account, the residual error between the instruments is reduced to **1.46nm rms** wavefront.
- This level of error is well below prescribed accuracy of the ZYGO itself.

# PSF Monitoring



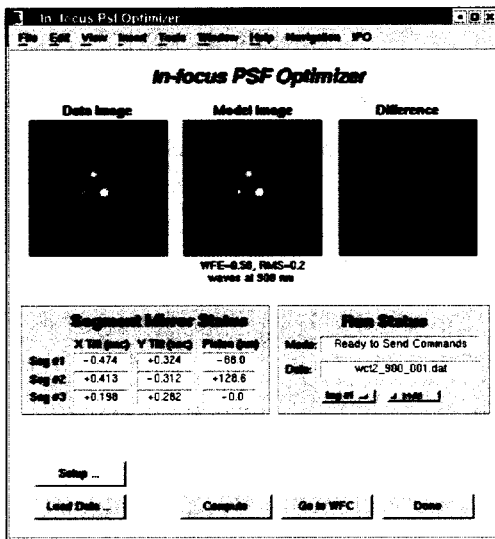
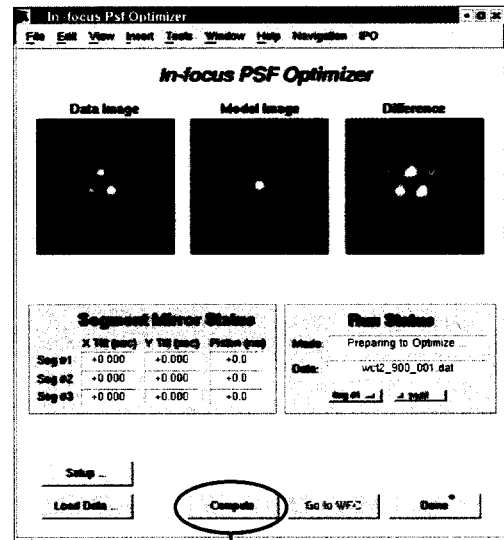
## In-focus PSF Optimizer (IPO)



- IPO uses in-focus images to measure low-order WF aberrations
  - "Prescription retrieval:" optimization function (Levenberg-Marquardt method) drives model parameters to match simulated images to data.
    - ◆ WCT-2 model includes segment piston, tip/tilt
    - ◆ Model can also include high resolution prior terms from other WFS and modeling sources.
    - ◆ Retrieved parameters are used to determine necessary controls

# Executive IPO Panel:

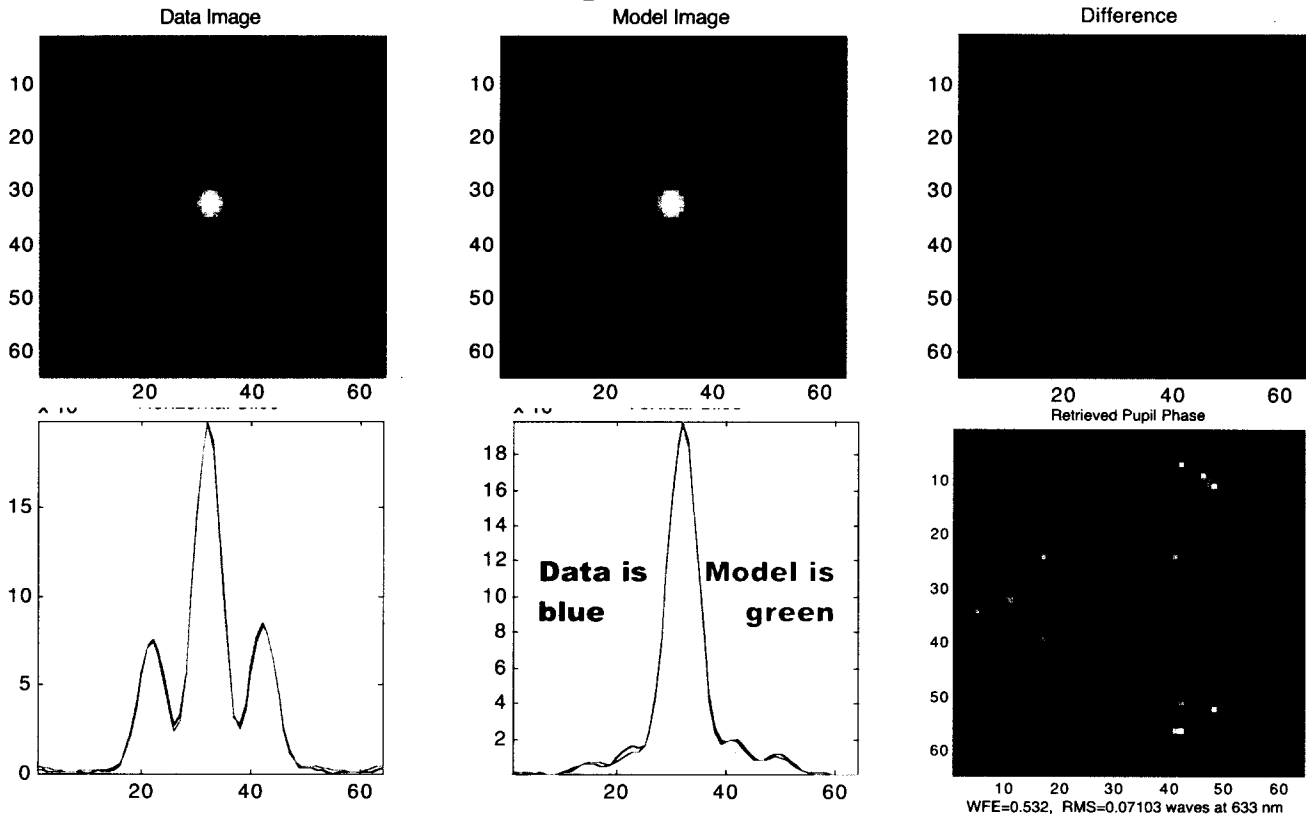
- Data image and perfect in-focus model image are displayed.
- Difference image shows piston error in Segs. 1 and 2.



- IPO detects -88 nm and +129 nm piston error in Segs. 1 and 2, respectively.
- Difference image shows excellent agreement between data image and IPO-model image.

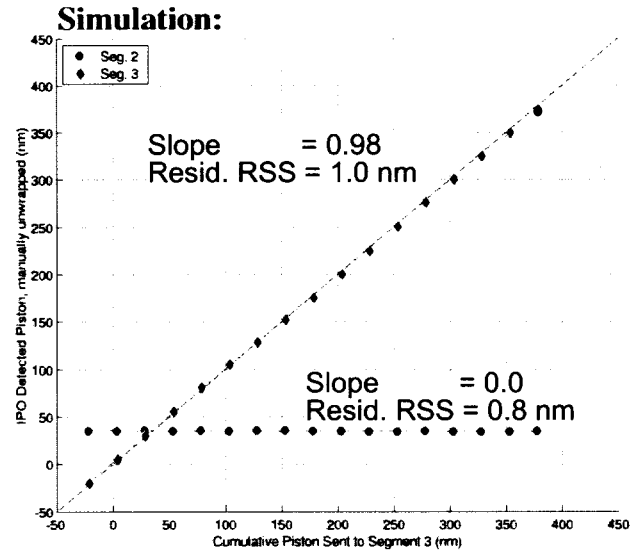
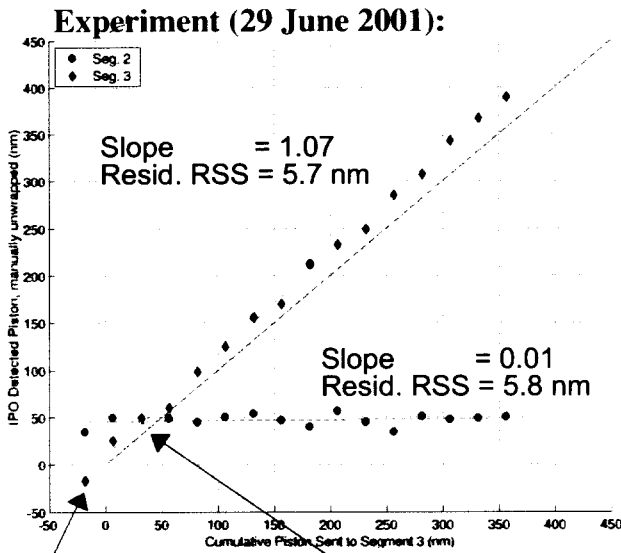


# Infocus Image: Magnified PSF, $\lambda = 633 \text{ nm}$



- WCT-2 data
  - 633 nm filter
  - 0.1 sec exposure time for min jitter
  - 250 frames
- Integer pixel shift-and-add
- PSF magnifier in place
- Blur  $\sigma_x = 0.84, \sigma_y = 1.74$  pixels
- Match = 0.27 RSS vs. total of 170

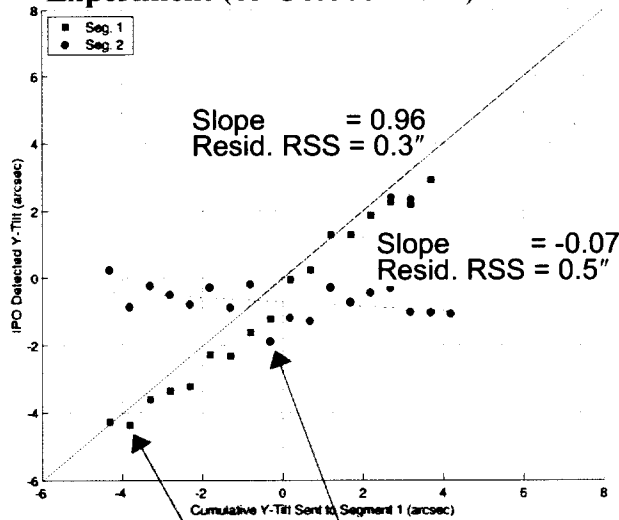
# Piston Accuracy with PSF Magnifier ( $\lambda=900$ nm)



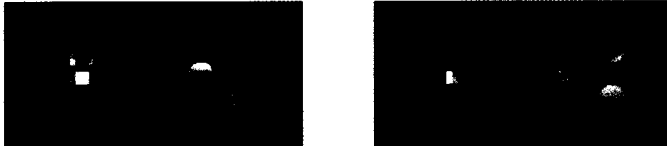
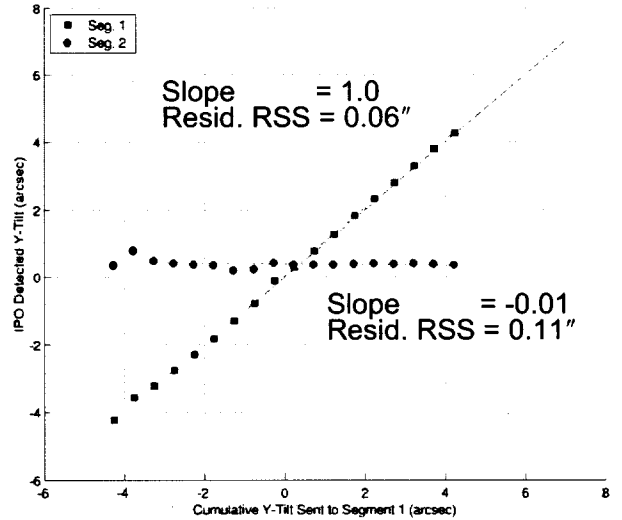
- ♣ Piston Seg. 3 in steps of +25 nm. Detected piston was manually unwrapped after 225 nm ( $\lambda/4$ ).
- ♣ Residual errors show ~6 nm piston detection uncertainty (RSS), which is on the same order as the 5 nm PZT

# Tip/tilt Accuracy, No PSF Magnifier ( $\lambda=900$ nm)

Experiment (05 October 2001):



## Simulation:

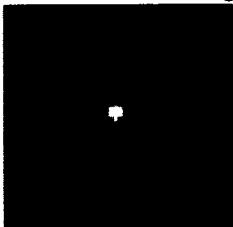


- Tilt Seg. 1 in steps of 0.5 arcsec.
- Residual errors show 0.3 to 0.5 arcsec. tilt detection uncertainty (RSS), which is larger than the PZT accuracy but consistent with simulations.

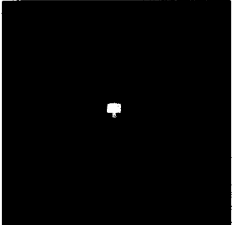
# 36 Segment NGST: “Symmetric ambiguity”



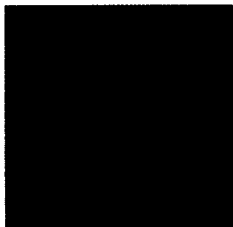
Simulated Data Image



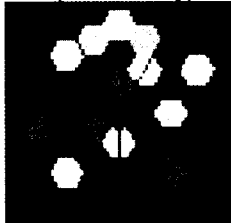
Model Image



Difference

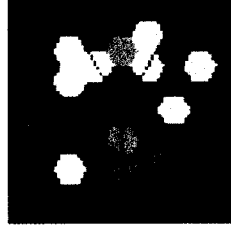


Injected Aberrations  
(Piston Only)



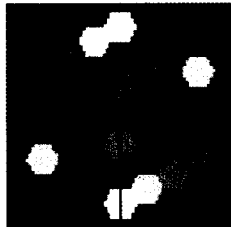
WFE (PV) = 0.24 waves

Retrieved Pupil Phase



WFE (PV) = 0.24 waves

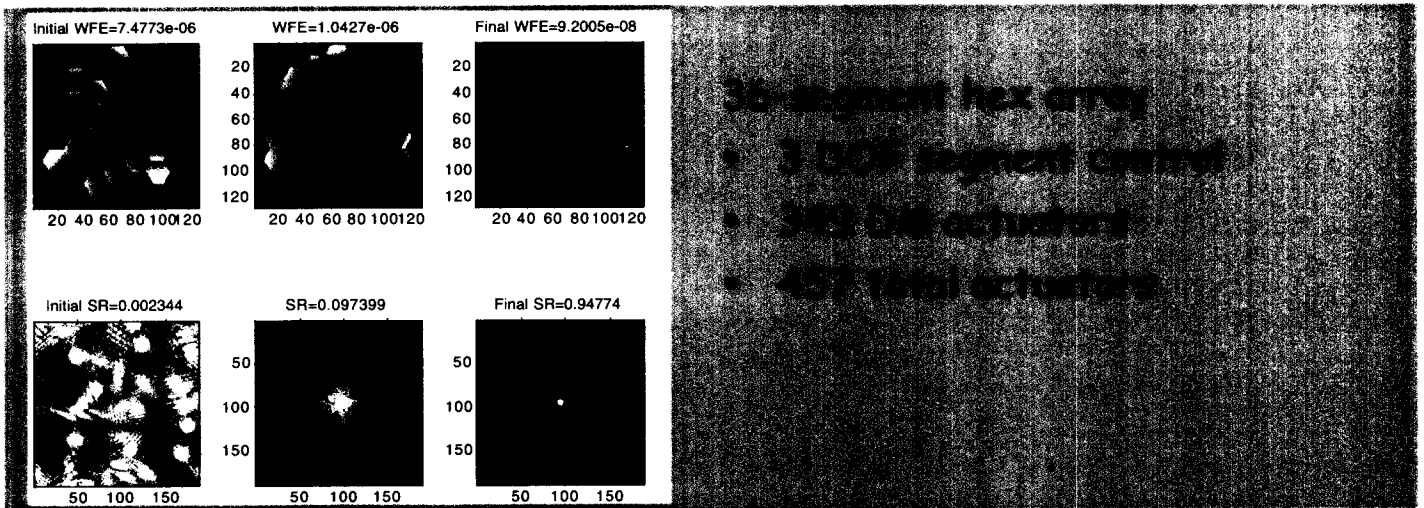
After Control



WFE (PV) = 0.27 waves

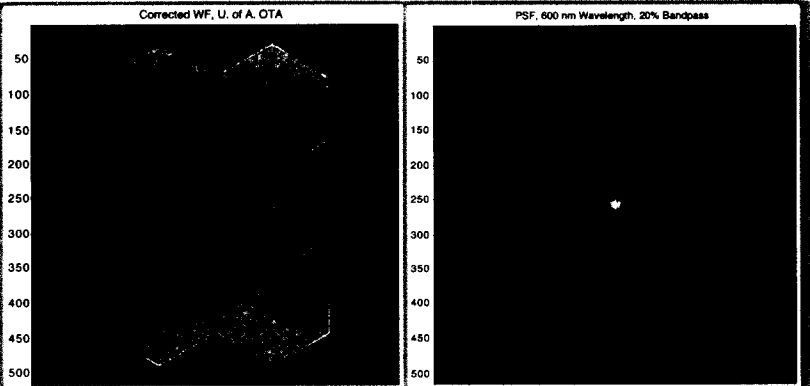
- In this example, IPO successfully identified the scalar WFE, but unsuccessfully measured the WF for control.
- Residual error after control is highly symmetric.
- Out of 100 trials:
  - 77% successfully ID'd scalar WF.
  - 70% successfully controlled the WF.
- Ambiguity can be broken in several ways

# Other Control Examples



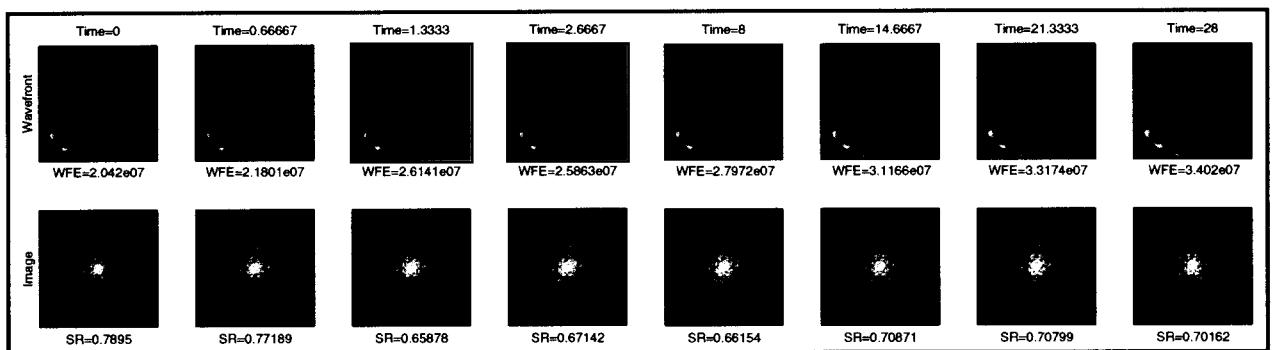
- 26-segment hex array
- 3.00% segment control
- 30% RMS distortions
- 40% total distortions

26-segment hex array  
 3.00% segment control  
 30% RMS distortions  
 40% total distortions

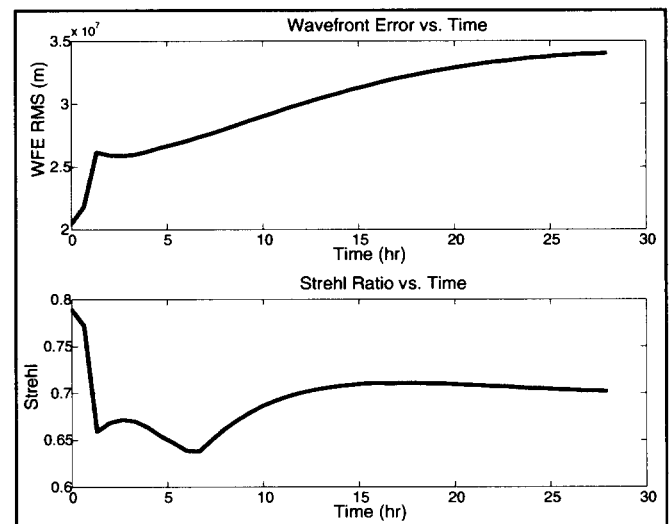




## Thermal WF Stability: No Thermal Control



- WF control performed at hottest attitude
  - SR = 79%
- 1 hr slew to coldest attitude
- Steady state reached 28 hours later
  - SR = 70%



## What We Have Demonstrated on WCT...



- Segment capture, alignment and coarse phasing
  - Capture range of mm
  - Accuracy of <100 nm DFS, <50 nm WLI
- Fine phasing of monolithic aperture using image-plane WFS and DM control
  - Capture range of several waves P-V
  - WFS repeatability of ~6 nm RMS, much better at low spatial frequencies
  - WFC performance to ~30 nm RMS scored at PSF
- Fine phasing of sparse segmented aperture using image-plane WFS, with segment and DM control
  - WFC performance to ~50 nm RMS scored at PSF
- In-focus WFS&C for continuous PSF monitoring and control
- Routine, robust operation of most control modes